Natural polynomials for Kerr quasinormal modes

Lionel London and Michelle Foucoin
King's College London, Strand, London WC2R 2LS, United Kingdom

(Received 2 January 2024; accepted 23 September 2025; published 4 February 2026)

We present a polynomial basis that exactly tridiagonalizes Teukolsky's radial equation for quasinormal modes. These polynomials naturally emerge from the radial problem, and they are "canonical" in that they possess key features of classical polynomials. Our canonical polynomials may be constructed using various methods, the simplest of which is the Gram-Schmidt process. In contrast with other polynomial bases, our polynomials allow for Teukolsky's radial equation to be represented as a simple matrix eigenvalue equation. We expect that our polynomials will be useful for better understanding the Kerr quasinormal modes' properties, particularly their prospective spatial completeness and orthogonality. We show that our polynomials are closely related to the confluent Heun and Pollaczek-Jacobi type polynomials. Consequently, our construction of polynomials may be used to tridiagonalize other instances of the confluent Heun equation. We apply our polynomials to a series of simple examples, including: (1) the high accuracy numerical computation of radial eigenvalues, (2) the evaluation and validation of quasinormal mode solutions to Teukolsky's radial equation, and (3) the use of Schwarzschild radial functions to represent those of Kerr. Along the way, a potentially new concept, "polynomial/nonpolynomial duality," is encountered and applied to show that some quasinormal mode separation constants are well approximated by confluent Heun polynomial eigenvalues. We briefly discuss the implications of our results on various topics, including the prospective spatial completeness of Kerr quasinormal modes.

DOI: 10.1103/nn8t-p14d

I. INTRODUCTION

The results of single black hole (BH) perturbation theory have proved widely useful to gravitational wave astronomy [1–10]. Most famously, the aftermath of binary black hole coalescence is expected to be a perturbed Kerr BH that rings down, radiating away its perturbation, predominantly in the form of damped oscillatory modes [11–18]. The related *ringdown* radiation is of practical relevance to many aspects of gravitational wave astronomy, from the construction of signal models, to the ongoing search for new physics [3,7–10,17–24]. Concurrently, ringdown radiation has inspired varied activity in gravitational wave theory, from efforts to understand BH nonlinearity, to emerging developments in the time-dependent perturbation theory of single BHs [25–29]. These efforts, among many others, aim to prepare gravitational wave science for a future in which high-precision ringdown measurements may point the way to a more complete understanding of gravity [30,30–37]. There is, therefore, good reason to think that a deeper practical understanding of linearly perturbed Kerr BHs is of use.

The present work is concerned with answering a number of questions regarding the mathematical structure and practical use of gravitational wave ringdown. Ringdown is comprised of quasinormal modes (QNMs), which are the analog of normal modes for dissipative systems [38–40]. Here, they will be treated under the Teukolsky formalism, where the field equations are separable, and where the QNMs are the joint point spectra of Teukolsky's *radial* and *angular* equations [12–16,41]. In this context, the present work addresses the following questions about Kerr QNMs.

What is the nature of the overtone label?—Not long after the pioneering work of Teukolsky, Press, and many others on linear perturbations of the Kerr geometry, Leaver lead the development of analytic methods for computing the QNM's functional dependence (i.e., in space and time) and mode numbers [15,42,43]. Since then, there has been tremendous progress in understanding the mathematical structure of Kerr QNMs [16,44–53]. For example, analysis of the gravitational field equations confers that QNMs are described by four mode numbers, one for each spacetime dimension [15,16]. In any asymptotically valid spacetime coordinates, these are $\tilde{\omega}_{\ell mn}$ (time), ℓ (polar angle), m (azimuthal angle), and n (radius). The polar mode number, ℓ, is unavoidably linked to the eigenvalues of Jacobi polynomials [54–56]. In this sense, the Jacobi polynomials are *natural* to the QNM problem. Regarding the azimuthal angle ϕ, this is similarly true of the monomials, ζ^m, where $\zeta = e^{i\phi}$. In contrast, the radial mode number, most commonly referred to as the "overtone" index,[1] has evaded rudimentary explanation.

Here, the overtone index is demonstrated to be closely related to the order parameter inherent to the confluent Heun polynomials [57–62]. Concurrently, it is observed, perhaps for the first time, that the confluent Heun polynomials exhibit a kind of "polynomial/nonpolynomial duality," where finite sets of confluent Heun polynomials are necessarily paired with an infinite set of nonpolynomial functions.

Is a simple spectral solution to Teukolsky's radial equation possible?—It was pointed out in Ref. [54] (hereafter Paper I) that there exists a scalar product for which Teukolsky's radial equation, while non-Hermitian [63–68], is self-adjoint and that this scalar product enables the direct application of Sturm-Liouville theory [69–72]. The scalar product's weight function coincides with the Green's function approach to QNMs pioneered by Leaver,[2] and the deformed Jacobi weight known for Pollaczek-Jacobi polynomials [43,54,73]. One use of the scalar product is to represent Teukolsky's radial equation as a simple linear matrix equation [74].

While many studies have developed matrix representations of Teukolsky's radial problem (e.g., [75–79]), the scalar product presented in Paper I was perhaps the first to result in matrix representations that are explicitly symmetric and tridiagonal, meaning that all physically relevant information is encoded in the diagonal and upper-diagonal matrix elements. Tridiagonal matrices are known to have a number of favorable properties; e.g., they are well-developed methods to study their asymptotic structure [73,80,81], and the classical properties of related polynomials enable efficient numerical methods [73,82,83]. To arrive at a tridiagonal representation of Teukolsky's radial equation, it was postulated that there may exist a basis of problem-specific, or "natural," polynomials.

Here, it is numerically shown that there do indeed exist unique classical-like polynomials that exactly tridiagonalize Teukolsky's radial equation. Therefore, the resulting method of the solution to the QNM's radial problem is spectral in the simplest possible way: widely available linear algebra packages may be used to explicitly diagonalize the problem, simultaneously yielding eigenvalues and eigenfunctions. The polynomials in question will be referred to as "canonical confluent Heun polynomials"; numerical examples are provided.

Is deeper analytic understanding possible?—Leaver's algorithm for computing the QNMs' functions and mode numbers has influenced many studies, particularly those of the QNM frequencies, $\tilde{\omega}_{\ell mn}$ [41,66,84]. Concurrently, methods such as the Wentzel-Kramers-Brillouin and eikonal approximations have supported advances in the analytic understanding of QNM's behavior in certain limits, e.g., very high BH spins, and/or very large values of ℓ [48,49,49]. Recently, there has been progress in understanding the pseudospectral stability of the QNM frequency spectrum [85–89]. Amid this activity, a number of related questions have remained open. These include: Do the QNMs' radial dependence have an underlying structure that is polynomial? Is it heuristically accurate to think of the radial mode number, n, as being the order of an underlying polynomial object, in the same way that ℓ are related to the order of a Jacobi polynomial?

Here, the QNMs' radial functions are shown to be generally nonpolynomial in nature, but potentially well approximated by a confluent Heun polynomial of order given by $n + 1$. A simple procedure for quantifying the approximate polynomial nature of a QNM's radial function is presented.

Are the QNMs spatially complete?—There has been a significant amount of research into the question of QNM completeness.[3] Some references appear at tension regarding whether the radial field equation is self-adjoint and therefore whether or not QNMs radial functions may be complete. This apparent tension arises from the fact it is insufficient to label a differential equation as non-self-adjoint, without additional statements about the coordinate domain, boundary conditions, and related bilinear form (e.g., inner or scalar product). For example, Refs. [39,85,90] describe analogs of the radial field equation as non-self-adjoint; however, akin to Refs. [26,91,92], a key result of Paper I was the construction of a radial scalar product *such that* the equation is self-adjoint.

Here, this scalar product is used to show that each QNM's radial function may be a member of an *orthonormal basis*. This new result places our understanding of the QNM's radial functions on the same footing as their angular functions [41,56,93,94]. In particular, it was shown in Ref. [56] that each QNM's angular function is a member of a basis and that the properties of all such angular bases

[1]The use of overtone is known to be somewhat of a misnomer; e.g., acoustic overtones have higher frequencies compared to a fundamental resonant frequency. In contrast, QNM overtones are known to have slightly lower frequencies (but higher damping rates) compared to the $n = 0$, or fundamental, QNMs.

[2]The radial equation studied here is the same studied by Leaver [15]. Forthcoming numerical results are ultimately equivalent to those from Leaver's series solution. However, truncations of Leaver's series solution (the infinite dimensional problem) should not be confused with the canonical polynomials presented in Sec. V, which are used to frame a finite dimensional problem in Sec. VI.

[3]A sequence of functions is complete (i.e., is a basis) if any piecewise continuous function on the same domain can be exactly expressed as a linear combination of sequence elements. It is a standard result in Sturm-Liouville theory and functional analysis that self-adjoint differential operators have complete eigenfunctions.

lead to the conclusion that the angular functions, namely the spheroidal harmonics with different QNM frequencies, are isomorphically equivalent to the spherical harmonics and therefore complete. The present work takes a first step towards an analogous conclusion for the QNM's radial functions: it is shown that change-of-basis matrices between Kerr and Schwarzschild are approximately diagonal, implying that they may be isomorphically equivalent. This communicates that, for a large range of BH spins, the radial functions of Kerr may be efficiently represented using those of Schwarzschild.

This result and its consequences may be particularly relevant for the formulation of a time-dependent perturbation theory for BHs, which presently requires the rather strong assumption that QNMs are spatially complete [26–29].

II. SCOPE AND ORGANIZATION

A. Scope

The focus of this article will be on linear order curvature perturbations of isolated Kerr BHs, as framed by Teukolsky, Press, and Leaver [12–15,42]. The related version of Einstein's equations, namely Teukolsky's equation, is well known to be non-Hermitian [66,90], and in that context, this work comments on select aspects of the problem that are shared with Hermitian problems: symmetric matrix representations, orthogonality, and the potential completeness of eigenspaces [26,54,56,95]. While this article discusses only gravitational perturbations (i.e., those with spin-weight $s = \pm 2$), all calculations present make no explicit assumption about spin-weight and, in most cases, have been verified to work with other physically relevant spin weights, namely $|s| \leq 2$. The authors do not aspire to the language of formal mathematical rigor; in place of theorems and lemmas, arguments are presented as needed, and the most technical of these are left to references. Numerical results will use QNM frequencies due to their physical relevance; however, this article's results use a framework that applies to any *single frequency*. The concurrent treatment of all QNM frequencies is left to future work. The unit convention, $G = c = 1$, will be used throughout.

B. Organization

This article is organized as follows. In Sec. III, a schematic background of single BH perturbations is provided, culminating in the definition of the QNM's radial eigenvalue problem and a brief review of Paper I. In Sec. IV, the QNM's radial eigenvalue problem is treated with confluent Heun polynomials. This section concludes with a discussion of the confluent Heun polynomials' pros and cons. In Sec. V, this article's central result, namely the *canonical confluent Heun polynomials*, is introduced. In Sec. VI, the canonical confluent Heun polynomials are shown to tridiagonalize Teukolsky's radial equation. In Sec. VII, numerical results are presented to demonstrate the canonical confluent Heun polynomials' end-to-end use. There, we note that, due to the known asymptotic properties of the QNMs radial functions' series solution, most truncated matrix representations of the radial problem will result in *spectral pollution* [39,96–100]. In Sec. VIII, the results of the preceding sections are discussed in the context of past and future work.

III. PRELIMINARIES

A. Observables and perturbative quantities

A gravitational wave observatory will detect a linear combination of the two strain polarizations present in Einstein's general relativity, h_+ and $h_\times$ [101]. We may parametrize each using Boyer-Lindquist coordinates $\{t, r, \theta, \phi\}$, where, asymptotically far from a radiating source, t may be defined to measure time elapsed for an observer, r the luminosity distance, and (θ, ϕ) the usual spherical polar angles [102]. Since all θ dependence is in the form of $u = \cos(\theta)$, u will henceforth be used [15].

From the perspective of Teukolsky's equation, it is convenient to work with the curvature scalar ψ_4, which is related to the strain polarizations via

$$h = h_+ - ih_\times \tag{1a}$$

$$= \int_{-\infty}^{t} \int_{-\infty}^{t'} \psi_4(t'', r, u, \phi) dt'' dt'. \tag{1b}$$

In Eq. (1), ψ_4 is the fifth scalar of the Weyl tensor in the Newman-Penrose formalism [103]. It is a field of spin-weight, $s = -2$, and encodes all relevant information about gravitational radiation [103–106]. For a single isolated BH, the rescaled Weyl scalar,

$$\psi = -(r - iau)^{-4} \psi_4, \tag{2}$$

satisfies Teukolsky's equation [12–14]. In Eq. (2), a is the BH spin magnitude divided by the BH mass. Schematically, if we denote the second-order linear partial differential operator within Teukolsky's equation as $\mathcal{L}_{tru\phi}$, then for isolated black holes

$$\mathcal{L}_{tru\phi} \psi = 0. \tag{3}$$

Since $\mathcal{L}_{tru\phi}$ has partial derivatives on each spacetime coordinate, the solutions ψ are waves [13].

B. Quasinormal modes

The QNMs of an isolated Kerr BH comprise a sequence of solutions to Eq. (3) that are ingoing waves at the BH horizon and purely outgoing radiation towards spatial infinity [13,15]. These conditions on a QNM's phase velocity are known to constrain the functional form of ψ

by defining the allowed radial behavior asymptotically near the event horizon and spatial infinity [12,15,41].

An individual QNM has spatiotemporal dependence given by the product of four functions,

$$\psi \propto R(r)S(u)e^{-i\tilde{\omega}t}e^{-im\phi}. \tag{4}$$

In Eq. (4), $R(r)$ will be referred to as simply a "radial function" and $S(u)$ a spheroidal harmonic [13]. Both are *implicitly parametrized* by the field's spin weight, s, as well as the azimuthal and temporal mode numbers, m and $\tilde{\omega}$, respectively. For given values of $\tilde{\omega}$ and m, the study of possible solutions for each $R(r)$ and $S(u)$ result in two additional mode numbers, n and ℓ, where ℓ is known to be closely related to the order of Jacobi polynomials [54–56]. One goal of the present work is to provide an analogous mathematical understanding of the colloquially named overtone number, n.

In Eq. (4), $\tilde{\omega} = \omega - i/\tau$ is a complex valued QNM or "ringdown" frequency, and τ must be positive for time domain stability of the BH [12,15,107]. Consequently, in the time domain, each QNM is a damped sinusoid with central frequency ω and damping time τ. Teukolsky's equation constrains the functional form of each QNM, and the details of the perturber constrain its overall excitation amplitude [43,46].

Furthermore, application of Eq. (4) to Teukolsky's equation yields that Eq. (3) separates (with separation constant A) into

$$\mathcal{L}_u S(u) = -AS(u), \tag{5a}$$

$$\mathcal{L}_r R(r) = +AR(r). \tag{5b}$$

Henceforth, Eqs. (5a) and (5b) will be referred to as Teukolsky's angular and radial equation, respectively. They are eigenvalue equations, where $-A$ and $+A$ are the respective complex valued[4] eigenvalues [42,54,56,108]. Therefore, $S(u)$ and $R(r)$ are the respective eigenfunctions. In Eq. (5), $\mathcal{L}_u$ and $\mathcal{L}_r$ are second-order linear differential operators that will be referred to as Teukolsky's angular and radial operators, respectively. Each implicitly depends on s, m, and $\tilde{\omega}$, as well as the BH mass M, and spin $a = |\vec{J}|/M$.

Considered on their own, i.e., outside of the explicit physical context described thus far where $\tilde{\omega}$ is assumed to be a QNM frequency, Eqs. (5a) and (5b) are known to have a discrete space of eigenfunctions, which may be labeled in ℓ' and n', respectively [15,109]. Their eigenvalues implicitly inherit these labels,

$$\mathcal{L}'_u S_{\ell'}(u) = -A_{\ell'} S_{\ell'}(u), \tag{6a}$$

$$\mathcal{L}'_r R_{n'}(r) = +A_{n'} R_{n'}(r). \tag{6b}$$

Equations (6a) and (6b) hold for *any* frequency parameter $\tilde{\omega}'$ that is independent of ℓ' and n'. Since $\mathcal{L}_u$ and $\mathcal{L}_r$ depend on the frequency parameter, they are also primed in Eq. (6). It is *only* for the QNM frequencies that $A_{\ell'} = A_{n'} = A$, and Eq. (5) is recovered. Since ℓ' and n' are independent, for any one QNM frequency, there will be only one value of ℓ' and one value of n' such that $A_{\ell'} = A_{n'}$. These special labels are those for which $\ell' = \ell$ and $n' = n$. For these reasons, the QNM frequencies and their separation constants are often labeled with spatial mode numbers, i.e., $\tilde{\omega}_{\ell mn}$ and $A_{\ell mn}$, respectively [16,17,32,84]. As a result, the QNMs are a nontrivial infinite sequence, wherein each element satisfies Eq. (6) with a nominally distinct frequency parameter, $\tilde{\omega}' = \tilde{\omega}_{\ell mn}$ [56].

An example of the angular and radial eigenvalue distributions is shown in Fig. 1. There, the typical qualitative features of each distribution are shown: the angular eigenvalues, $A_{\ell'}$, will typically be spaced horizontally along the real axis, and the radial eigenvalues, $A_{n'}$, will vary most strongly in their imaginary part. Since the case shown has been constructed using a QNM frequency, there will be a single coincident eigenvalue, which is the one of physical interest [i.e., the one compatible with the construction of [Eq. (5)].

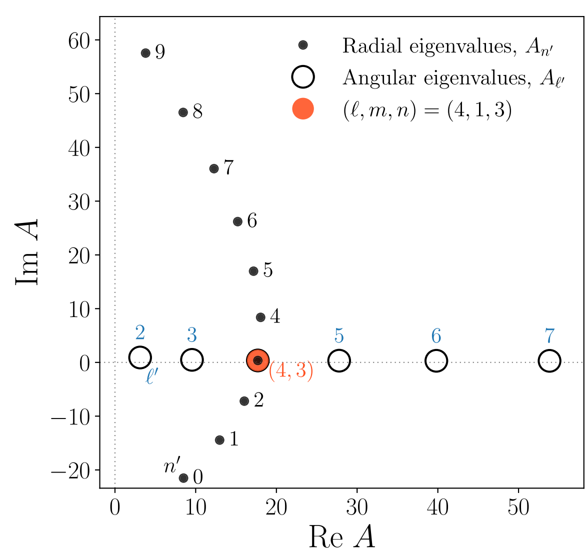

FIG. 1. Distributions of radial (black dots) and angular eigenvalues (open circles) for $s = -2$, BH dimensionless spin $a/M = 0.7$, and the $(\ell, m, n) = (4, 1, 3)$ QNM with $M\tilde{\omega}_{413} = 0.8545 - 0.6305i$. Since both eigenvalue distributions have been computed with a QNM frequency, they have one coincident value corresponding to $(\ell', n') = (\ell, n) = (4, 3)$. Radial eigenvalues shown have been computed using the results of the current work and verified using Leaver's method [15].

[4]The complex nature of the eigenvalues is a consequence of the fact that Eqs. (5a) and (5b) have complex valued terms. It will be seen in Eq. (14) that this coincides with a nonconjugate symmetric scalar product.

C. Notation

For convenience of notation, QNM frequencies will henceforth be referred to as $\tilde{\omega}_{\ell mn}$, and $\tilde{\omega}$ will refer to an arbitrary frequency parameter. The related radial eigenvalue relation will be referred to simply as

$$\mathcal{L}_r R(r) = A R(r), \tag{7}$$

where it is implicitly understood that the eigenvalues, A, and eigenfunctions, $R(r)$, are elements of that equation's discrete spectra. A transformed version of the radial equation will be encountered shortly. At that time, the same notational strategy will be used.

D. A radial scalar product

The angular equation, Eq. (6a), is well known to be of the Sturm-Liouville type (i.e., $\mathcal{L}_u$ is self-adjoint) [54,56,72,110]. Consequently, its eigenfunctions, $S_{\ell'}(u)$, are complete[5] and orthogonal with respect to a scalar product, $\langle a|b\rangle$, defined by the integral of $a(u)b(u)$ on $u \in [-1,1]$. The application of this angular scalar product is fundamental to the use of spherical and spheroidal harmonics in gravitational wave theory and data analysis [8,101,112].

In contrast, the radial equation, Eq. (6b), is known to not explicitly be of the Sturm-Liouville type. This simply means that, in practice, the application of Sturm-Liouville theory must begin with the construction of a *weighted* scalar product, under which $\mathcal{L}_r$ is self-adjoint [69,72,113]. Below, we provide a brief overview of the construction and evaluation of such a radial scalar product. We refer the reader to Paper I for a complete pedagogical development.

Using the compactified radial coordinate,

$$\xi = (r - r_+)/(r_-), \tag{8}$$

and applying the QNMs' asymptotic boundary conditions via an appropriate rescaling,

$$R(r(\xi)) = \mu(\xi) f(\xi), \tag{9}$$

the radial problem is transformed so that the radial function of interest is now $f(\xi)$, and differential operator $\mathcal{L}_r$ becomes

$$\mathcal{L}_\xi = (\mathrm{C}_0 + \mathrm{C}_1(1-\xi)) \tag{10a}$$

$$+ (\mathrm{C}_2 + \mathrm{C}_3(1-\xi) + \mathrm{C}_4(1-\xi)^2)\partial_\xi \tag{10b}$$

$$+ \xi(\xi - 1)^2 \partial_\xi^2. \tag{10c}$$

[5] See Ref. [111] for a discussion of completeness in the context of single complex valued oblateness parameters (i.e., $a\tilde{\omega}$), and see Ref. [56] for related discussion of completeness in the QNM context, where oblateness parameters differ from mode to mode.

The operator $\mathcal{L}_\xi$ may be compactly written by defining the operator $\mathcal{D}_\xi$ to be the terms within Eqs. (10b) and (10c),

$$\mathcal{L}_\xi = (\mathrm{C}_0 + \mathrm{C}_1(1-\xi)) + \mathcal{D}_\xi. \tag{11}$$

Note that in Eq. (8), ξ maps $r \in [r_+, \infty)$ to $\xi \in [0,1)$, thereby compactifying the radial coordinate. In Eq. (9), $\mu(\xi)$ is comprised of factors related to the singular exponents of $\mathcal{L}_r$. Its explicit form is given in Eq. (12) of Paper I. In Eq. (10), C_0 through C_4 are complex valued constants determined by the BH mass M, the BH spin a, the mode numbers $\{\tilde{\omega}, m, l, n\}$, and the field's spin weight s:

$$\mathrm{C}_0 = -2am\tilde{\omega} - 2i\tilde{\omega}(-\delta + M(2s+1)) + \tilde{\omega}^2(\delta + M)(\delta + 7M), \tag{12a}$$

$$\mathrm{C}_1 = 8M^2\tilde{\omega}^2 + s(4iM\tilde{\omega} - 1) + 6iM\tilde{\omega} - 1 - (4M\tilde{\omega} + i)\frac{(am - 2M^2\tilde{\omega})}{\delta}, \tag{12b}$$

$$\mathrm{C}_2 = 4i\delta\tilde{\omega}, \tag{12c}$$

$$\mathrm{C}_3 = -2(s+1) + 4i\tilde{\omega}(M - \delta), \tag{12d}$$

$$\mathrm{C}_4 = s + 3 - 6iM\tilde{\omega} + \frac{i(am - 2M^2\tilde{\omega})}{\delta}, \tag{12e}$$

$$\delta = \sqrt{M^2 - a^2}. \tag{12f}$$

Lastly, note that none of C_0 through C_4 become zero when $a = 0$. As a result, Eq. (11) is of the confluent Heun type for both Schwarzschild and Kerr [54].

Together, Eqs. (8)–(12) allow the radial eigenvalue relation [Eq. (7)] to be rewritten as

$$\mathcal{L}_\xi f(\xi) = A f(\xi). \tag{13a}$$

The equivalent statement in standard bra-ket notation is

$$\mathcal{L}_\xi |f\rangle = A|f\rangle. \tag{13b}$$

In Eq. (13b), and henceforth, the use of bra-ket notation is consistent with the fact that $f(\xi)$ is a vector in space whose bilinear product is the radial scalar product of interest. The practical use of kets, e.g., $|\Phi\rangle$, and bras, $\langle\Phi|$, will be demonstrated in the context of the scalar product.

A scalar product between two smooth functions of ξ, $a(\xi)$ and $b(\xi)$, is defined as

$$\langle \mathrm{a}|\mathrm{b}\rangle = \int_0^1 \mathrm{a}(\xi)\mathrm{b}(\xi)\ \mathrm{W}(\xi) d\xi, \tag{14}$$

where $\mathrm{W}(\xi)$ is the product's *weight function*. In turn, $\mathrm{W}(\xi)$ is defined such that the operator, $\mathcal{L}_\xi$, is equal to its adjoint, $\mathcal{L}_\xi^\dagger$, with respect to the scalar product:

$$\begin{aligned}\langle a|\mathcal{L}_\xi b\rangle &= \langle \mathcal{L}_\xi^\dagger a|b\rangle \\ &= \langle \mathcal{L}_\xi a|b\rangle. \end{aligned} \tag{15}$$

Note that there is no conjugation in Eq. (14). As a result, Eq. (15)'s adjoint operator, $\mathcal{L}_\xi^\dagger$, does not involve complex conjugation.

By combining the definition of $\mathcal{L}_\xi$ [Eq. (10)] with the requirement of self-adjointness [Eq. (15)] and then applying integration by parts, it may be shown that

$$\mathrm{W}(\xi) = \xi^{\mathrm{B}_0}(1-\xi)^{\mathrm{B}_1} e^{\frac{\mathrm{B}_2}{1-\xi}}, \tag{16}$$

where constants B_0 through B_2 are

$$\mathrm{B}_0 = \mathrm{C}_2 + \mathrm{C}_3 + \mathrm{C}_4 - 1 \tag{17a}$$

$$\mathrm{B}_1 = -\mathrm{C}_2 - \mathrm{C}_3 - 2 \tag{17b}$$

$$\mathrm{B}_2 = \mathrm{C}_2. \tag{17c}$$

In practice, if the series expansion of two functions, $\mathrm{a}(\xi)$ and $\mathrm{b}(\xi)$, exist and are known,

$$\mathrm{a}(\xi) = \sum_{j=0} \mathrm{a}_j \xi^j \quad \text{and} \quad \mathrm{b}(\xi) = \sum_{k=0} \mathrm{b}_k \xi^k, \tag{18}$$

then the scalar product may be evaluated as

$$\langle \mathrm{a}|\mathrm{b}\rangle = \sum_{j,k} \mathrm{a}_j \mathrm{b}_k \langle \xi^{j+k}\rangle. \tag{19}$$

In Eq. (19), $\langle \xi^{j+k}\rangle$ are called *monomial moments* [83]. Using the definition of the weight function, it has been observed (e.g., [43,70,114]) that each monomial moment $\langle \xi^p\rangle$ can be evaluated using the gamma function, $\Gamma(x)$, and the Tricomi confluent hypergeometric function, $U(x,y,z)$,

$$\begin{aligned}\langle \xi^p\rangle &= e^{\mathrm{B}_2}\Gamma(\mathrm{B}_0 + p + 1) \\ &\quad \times U(1 + \mathrm{B}_0 + p, -\mathrm{B}_1, -\mathrm{B}_2). \end{aligned} \tag{20}$$

Equations (19) and (20) enable the scalar product to be evaluated for complex values of B_0, B_1, and B_2 via the standard analytic continuations of $\Gamma(x)$ and $U(x,y,z)$ [54].

E. Confluent Heun polynomials

In many areas of physics, polynomial solutions to a system's equations of motion play an important role in describing that system's natural modes [41,55,56,115]. For the QNM's radial problem [Eq. (13)], one approach to understanding polynomial solutions begins by studying the differential part of $\mathcal{L}_\xi$, namely,

$$\mathcal{D}_\xi = (\mathrm{C}_2 + \mathrm{C}_3(1-\xi) + \mathrm{C}_4(1-\xi)^2)\partial_\xi + \xi(\xi-1)^2\partial_\xi^2. \tag{21}$$

This operator defines polynomials that satisfy a two-parameter eigenvalue problem,

$$\mathcal{D}_\xi|y_{pk}\rangle = (\lambda_{pk} + \mu_p \xi)|y_{pk}\rangle, \tag{22a}$$

where

$$\mu_p = p(p + \mathrm{C}_4 - 1). \tag{22b}$$

In Eq. (22a), λ_{pk} is the eigenvalue, and the linear factor, μ_p, is required for the polynomials, $|y_{pk}\rangle$, to terminate after $p+1$ terms [54,57]. For each polynomial order p, there are $p+1$ solutions for λ_{pk} that allow for termination [54,58]. The label k heuristically orders these solutions according to the imaginary part of, $\mathrm{Im}\,\lambda_{pk}$ [54]. Since Eq. (22a) is a confluent Heun equation, $|y_{pk}\rangle$ comprise a class, or multiplex, of order-p confluent Heun polynomials [57].

The ostensibly unusual (two parameter) nature of Eq. (22a) is a consequence of $\mathcal{D}_\xi$'s polynomial coefficient functions [Eq. (21)]. For example, when acting upon any polynomial of order p, $\xi(1-\xi)^2\partial_\xi^2$ will generally result in a polynomial of order $p+1$. The same is true of $(\mathrm{C}_2 + \mathrm{C}_3(1-\xi) + \mathrm{C}_4(1-\xi)^2)\partial_\xi$. Therefore, $\mathcal{D}_\xi$ generally increases the order of polynomials by one, which precludes the usual eigenrelation, where order is preserved.

A consequence of the multiparameter eigenrelation is that the confluent Heun polynomials do not obey exactly the same kind of orthogonality found in the classical polynomials. This may be seen by noting that, like $\mathcal{L}_\xi$, $\mathcal{D}_\xi$ is self-adjoint with respect to the scalar product,

$$\langle y_{pk'}|\mathcal{D}_\xi y_{pk}\rangle = \langle \mathcal{D}_\xi y_{pk'}|y_{pk}\rangle. \tag{23}$$

Applying the eigenvalue relationship, Eq. (22), to both sides of Eq. (23) yields

$$(\lambda_{pk} - \lambda_{p'k'})\langle y_{p'k'}|y_{pk}\rangle = (\mu_{p'} - \mu_p)\langle y_{p'k'}|\xi|y_{pk}\rangle. \tag{24}$$

For self-adjoint and single-parameter eigenvalue problems, the right-hand side of Eq. (24) is identically zero, resulting in the well-known orthogonality of eigenfunctions with unique eigenvalues [74,115]. Since μ_p is not generally zero, *only* the polynomials of like order (i.e., $\mu_{p'} - \mu_p = 0$) are orthogonal,

$$\langle y_{pk'}|y_{pk}\rangle = \delta_{k'k}. \tag{25}$$

In Eq. (25), $|y_{pk}\rangle$ are normalized, i.e., scaled such that $\langle y_{pk}|y_{pk}\rangle = 1$ [54].

It was observed in Paper I that λ_{pk} are nondegenerate across physically relevant values of BH mass and spin. Consequently, each $p+1$ dimensional vector space of polynomials y_{pk} is expected to be a basis, meaning that the identity operator for order-p polynomials may be written as

$$\mathbb{I}_p = \sum_{k=0}^{p} |y_{pk}\rangle\langle y_{pk}|. \tag{26}$$

However, since each basis for order-p polynomials spans all previous bases, the total set of confluent Heun polynomials satisfying Eq. (22a) is redundant, or rather *overcomplete* [116].

Lastly, the overcompleteness of the confluent Heun polynomials does not imply that it is trivial to use them as a basis for general solutions to the QNM radial problem. Doing so presents two challenges that we will discuss in upcoming sections. The first challenge is that each fixed-order confluent Heun polynomial basis need not have well-ordered expansion coefficients, meaning that there is *not necessarily* an order to how much each polynomial contributes to a radial expansion. This challenge will be discussed in the upcoming section, Sec. IV.

The second challenge is that the matrix representation of, e.g., $\mathcal{L}_\xi$ in a finite dimensional basis need not have *exactly the same spectra* as its infinite dimensional counterpart (i.e., there may appear modes that are purely the effect of truncation) [96]. This challenge will be revisited in Sec. VII.

IV. THE RADIAL PROBLEM WITH CONFLUENT HEUN POLYNOMIALS

The properties of confluent Heun polynomials have three implications for each QNM's radial problem [Eq. (13b)].

The first is that the radial problem, when represented in a basis of order-p confluent Heun polynomials, may be written simply, with a *deformation parameter*,

$$\alpha_p = \mu_p - \mathrm{C}_1, \tag{27}$$

that determines the size of all off-diagonal terms. Concurrently, off-diagonal terms are proportional to $\langle y_{pk'}|\xi|y_{pk}\rangle$, meaning that, for nonzero α_p, the matrix representation of the radial problem may not be approximately diagonal in the sense that elements do not necessarily decrease far away from $k' = k$.

The second implication is that, due to properties of α_p, a kind of *duality* exists in the radial problem's solution space. Most simply, if $\alpha_p = 0$ and p is a non-negative integer, then $p+1$ solutions will be polynomials, while the remaining infinity of solutions will be infinite series.

The final implication is that the physical QNMs will not, generally, be approximately polynomial in nature. Along with the aforementioned duality, this implies that there will typically be two, sometimes overlapping, sectors of solution space. It happens that this concurrently highlights practical issues that arise when attempting to approximate a function with an arbitrary fixed-order polynomial basis.

While these implications provide an instructive reference for the basic properties of nonpolynomial solutions to the radial equation, they also motivate the development of a basis comprised of uniquely ordered polynomials. That is the topic of the next section. For now, the radial problem with confluent Heun polynomials is to be discussed in more detail.

A. The radial problem

Any order-p confluent Heun polynomial basis may be used to approximate the radial problem,

$$\mathbb{I}_p \mathcal{L}_\xi \mathbb{I}_p |f\rangle = A \mathbb{I}_p |f\rangle, \tag{28a}$$

$$\hat{L}_p{}^{(\mathrm{cH})} \vec{\mathrm{f}} = A \vec{\mathrm{f}}. \tag{28b}$$

In Eq. (28a), insertion of the identity operator [Eq. (26)] signals that, e.g., $|f\rangle$ will be represented in the basis of order-p confluent Heun polynomials. In Eqs. (28b), (26) has been applied, and it has been recognized that the equation is equivalent to a matrix eigenvalue equation, where $\hat{L}_p{}^{(\mathrm{cH})}$ is a $(p+1)\times(p+1)$ matrix with elements,

$$L_{p,k'k}{}^{(\mathrm{cH})} = \langle y_{pk'}|\mathcal{L}_\xi|y_{pk}\rangle, \tag{29}$$

and $\vec{\mathrm{f}}$ has elements $\langle y_{pk}|f\rangle$.

In many cases, $\hat{L}_p{}^{(\mathrm{cH})}$ will have many off-diagonal terms. This may be understood by recalling that $\mathcal{L}_\xi = (\mathrm{C}_0 + \mathrm{C}_1[1-\xi]) + \mathcal{D}_\xi$, i.e., [Eq. (11)], and then applying the confluent Heun polynomial eigenvalue relationship to $\langle y_{pk'}|\mathcal{L}_\xi|y_{pk}\rangle$, yielding

$$\langle y_{pk'}|\mathcal{L}_\xi|y_{pk}\rangle = (\mathrm{C}_0 + \mathrm{C}_1 + \lambda_{pk})\delta_{k'k} + \alpha_p \langle y_{pk'}|\xi|y_{pk}\rangle. \tag{30a}$$

In Eq. (30a), α_p is defined by Eq. (27).

If $\alpha_p = 0$, Eqs. (28b) and (30a) yield that the QNM separation constant is simply given by

$$A_{pk} = \mathrm{C}_0 + \mathrm{C}_1 + \lambda_{pk}. \tag{31}$$

If a QNM's radial functions are well approximated by a single confluent Heun polynomial, then Eq. (31) will be similarly approximate.

When $\alpha_p \neq 0$, the off-diagonal elements of $\hat{L}_p{}^{(\mathrm{cH})}$ will be proportional to $\langle y_{pk'}|\xi|y_{pk}\rangle$. It was found in Paper I that $|\langle y_{pk'}|\xi|y_{pk}\rangle|$ do not typically decrease in value as $|k'-k|$ increases. Consequently, $\hat{L}_p{}^{(\mathrm{cH})}$ will typically be neither band-diagonal nor approximately diagonal when $\alpha_p \neq 0$.

B. Polynomial/nonpolynomial duality

From inspection of Eq. (30a), it is clear that when $\alpha_p = 0$, $\hat{L}_p{}^{(\mathrm{cH})}$ is diagonal. This implies that $\hat{L}_p{}^{(\mathrm{cH})}$ may be *approximately diagonal* when $|\alpha_p| \ll 1$. In the case where $\alpha_p = 0$, a finite subset of the solution space will be comprised of polynomials, and the remainder will be an infinite set of nonpolynomial functions.

It happens that, when $\alpha_p \neq 0$, the solution space will typically be comprised of two qualitatively distinct sectors: some solutions will be approximately polynomial in the sense that their series expansions converge quickly after some particular term and other strongly nonpolynomial solutions whose series expansions converge relatively slowly (see, e.g., the asymptotic analysis in Ref. [39]). Henceforth, we refer to the presence of these two solution types as polynomial/nonpolynomial duality.[6]

This concept may be refined by defining *pseudopolynomial orders*, $p_\star^+$ and $p_\star^-$, such that $\alpha_{p_\star^\pm}$ is zero:

$$\alpha_{p_\star^\pm} = \mu_{p_\star^\pm} - \mathrm{C}_1 \tag{32a}$$

$$= p_\star^\pm (p_\star^\pm + \mathrm{C}_4 - 1) - \mathrm{C}_1 = 0. \tag{32b}$$

In Eq. (32b), $\mu_{p_\star^\pm}$ has been rewritten using Eq. (22b). Solving for $p_\star^\pm$, one finds that

$$p_\star^\pm = \frac{1}{2}\left[(1-\mathrm{C}_4) \pm \sqrt{4\mathrm{C}_1 + (1-\mathrm{C}_4)^2}\right]. \tag{33}$$

In what follows, $p_\star^+$ will be referred to as the *upper* pseudopolynomial order, and $p_\star^-$ will be referred to as the *lower* pseudopolynomial order.

For the moment, we are concerned with the implications of the pseudopolynomial orders on solutions to the radial problem [Eq. (28)], the QNMs radial functions, and the ultimate practicality of confluent Heun polynomial representations for nonpolynomial problems.

Equation (33) implies a number of simple relationships between α_p, μ_p, $p_\star^+$, and $p_\star^-$. For example, Eq. (33) may be used to show that

$$p_\star^+ + p_\star^- = 1 - \mathrm{C}_4. \tag{34}$$

It also follows that $\mathrm{C}_1 = -p_\star^+ p_\star^-$. In terms of physical parameters [Eq. (12)], $p_\star^+$ and $p_\star^-$ are

$$p_\star^+ = -1 + 4iM\tilde{\omega}, \tag{35a}$$

$$p_\star^- = p_\star^+ - s - 2iM\tilde{\omega} - \frac{i(am - 2M^2\tilde{\omega})}{\delta}. \tag{35b}$$

[6]We expect polynomial/nonpolynomial duality to be related to the existence of quasibound states for $s = 0$ [117,118].

In Eq. (35) we have simplified Eq. (33) by adopting the strategy of Ref. [13] and holding that if x is a complex number, then, e.g., $\sqrt{-x^2} = ix$, rather than the generally correct value of $-ix\,\mathrm{sign}(\mathrm{Im}(x))$. The effect of this choice is to swap $p_\star^+$ with $p_\star^-$. Thus, it should be understood that Eqs. (35) and (33) are formally different.

Lastly, Eq. (33) allows α_p to be written as

$$\alpha_p = (p - p_\star^+)(p - p_\star^-). \tag{36}$$

From Eq. (34), three scenarios may be deduced for which the solution space includes a finite number of polynomials in addition to an infinity of nonpolynomials:

(i) The first scenario is that if $p_\star^+$ is a positive integer, then $p_\star^-$ typically will not be unless C_4 is a sufficiently negative integer.

(ii) The second scenario is simply that of the first, but with $p_\star^-$ being a positive integer and $p_\star^-$ having a fractional part.

(iii) In the remaining scenario *both* $p_\star^-$ and $p_\star^+$ are integers. In this case, it is possible for the solution space to support two sets of polynomials, each of different order, as well as an infinite number of nonpolynomial solutions.

Generally, neither $p_\star^+$ nor $p_\star^-$ will be positive integers for the QNMs, and their proximity to a positive integer will vary with different values of the overtone index, n. In particular, solutions to the QNM radial problem may only be closely associated with confluent Heun polynomials when $\tilde{\omega}_{\ell mn}$ are such that $p_\star^+$ or $p_\star^-$ is close to a positive integer according to

$$|\,\mathrm{Im}\, p_\star^\pm / \mathrm{Re} p_\star^\pm| \ll 1, \tag{37a}$$

and

$$p_\star^\pm - [\mathrm{Re} p_\star^\pm] \ll 1. \tag{37b}$$

In Eq. (37), $[x]$ denotes rounding to the nearest integer (e.g., $[3.1416] = 3$).

Table I provides examples of $p_\star^\pm$ for select QNM cases with mode numbers $(\ell, m) = (2, 2)$. Values of $p_\star^\pm$ have been defined using Eq. (33). It is observed that the QNM's $p_\star^+$ only very roughly tracks the overtone index, being approximately off by one for, e.g., $n = 2$, but off by significantly less than one for $n = 6$ and above. The case of the fundamental QNM, $n = 0$, demonstrates a general observation, namely that the $n = 0$ QNMs are typically not close to confluent Heun polynomial systems in that their $p_\star^\pm$ are not close to integers.

C. Polynomial noise

Since the QNMs $p_\star^\pm$ are typically complex valued, it is not guaranteed that using an order-p confluent Heun

TABLE I. Select pseudopolynomial orders, $p_\star^+$ and $p_\star^-$, for BH spin of $a/M = 0.7$ and QNM indices $(s, \ell, m) = (-2, 2, 2)$. Parameters for select QNM overtone numbers, n, are shown. Only even n are shown for brevity and results for odd n show the same qualitative trend [e.g., for $n = 13$, $(p_\star^+, p_\star^-) = (14.0178 + 0.0245i, 9.8469 + 1.6539i)$]. We do not show the result for $n = 8$, where further conditions are needed due to the appearance of nontraditional modes [41].

n	$p_\star^+$	$p_\star^-$
0	$1.3879 + 0.5964i$	$-0.6768 + 2.1304i$
1	$2.1725 + 0.5415i$	$-0.0230 + 2.0846i$
2	$2.9791 + 0.4394i$	$0.6490 + 1.9996i$
4	$4.6187 + 0.1537i$	$2.0152 + 1.7615i$
6	$6.2586 + 0.0743i$	$3.3816 + 1.6954i$
8	…	…
10	$11.0503 + 0.0551i$	$7.3742 + 1.6794i$
12	$13.0252 + 0.0344i$	$9.0198 + 1.6621i$
14	$15.0134 + 0.0152i$	$10.6765 + 1.6461i$
16	$17.0123 - 0.0004i$	$12.3420 + 1.6331i$
18	$19.0204 - 0.0084i$	$14.0152 + 1.6265i$
20	$21.0298 - 0.0007i$	$15.6895 + 1.6329i$

polynomial basis with, e.g., $p = \lfloor \max(|p_\star^+|, |p_\star^-|) \rfloor$ will yield an accurate representation of the radial problem. Worse, simply increasing the order of the confluent Heun polynomial basis (i.e., increasing p) does not necessarily result in a more precise representation. This may be understood as resulting from a basic limitation of approximation with fixed-order polynomial bases.

As a somewhat extreme but plausible example, consider the order-50 confluent Heun polynomial approximation of the number 1,

$$|1\rangle = \sum_{k=0}^{50} |y_{50,k}\rangle \langle y_{50,k}|1\rangle. \tag{38}$$

Each polynomial, $|y_{50,k}\rangle$, has 51 coefficients, and on the right-hand side of Eq. (38), values of $\langle y_{50,k}|1\rangle$ must conspire such that only constant terms survive the sum (as is required since 1 is a constant). In practice, finite precision means that the cancellations will not be exact. As a result, the net approximation will be contaminated by high frequency polynomial oscillations, or rather, *polynomial noise*.

Clearly, in this case it would be wise to represent $|1\rangle$ with the order-0 confluent Heun polynomial. This is consistent with the completeness of each confluent Heun polynomial fixed order basis: an order-p confluent Heun polynomial basis can exactly represent polynomials of the same order; while lower order polynomials may also be represented, their representation in polynomial bases of much larger order increases the likelihood of numerical noise.

Further, for nonpolynomial functions, it will not clear *a priori* which, if any, fixed order confluent Heun polynomial basis should be used. For example, since the QNMs' radial functions, $|f\rangle$, are generally nonpolynomial, one might attempt to apply a very large order confluent Heun polynomial representation,

$$|f\rangle = \sum_{k=0}^{P} |y_{Pk}\rangle \langle y_{Pk}|f\rangle, \tag{39}$$

where $P \gg 1$. In practice, the result would be contaminated by polynomial noise: all $\langle y_{Pk}|f\rangle$ would have to be given to arbitrarily high precision such that the sum's $(P+1)^2$ polynomial coefficients (i.e., there are $P+1$ polynomials and each with $P+1$ coefficients) add without significant contamination from round-off error.

In contrast, a basis of $P+1$ classical polynomials (i.e., with unique orders ranging from 0 to P) would only have $\frac{1}{2}(P+1)^2$ coefficients to total. More importantly, unlike the order-P confluent Heun polynomials, such a basis would have expansion coefficients (analogs of $\langle y_{Pk}|f\rangle$) that necessarily decrease as k increases, meaning that fewer than $\frac{1}{2}(P+1)^2$ coefficients may ultimately be of practical importance.

D. Towards canonical polynomials

Together, these ideas may be summarized as follows. Since an order-p confluent Heun polynomial basis is complete, it may be used to approximate the radial problem in a way that explicitly reduced to a polynomial solution in the limit that $\alpha_p = 0$. Further, it may be possible to treat general solutions of the radial problem perturbatively, where $\alpha_p = (p - p_\star^+)(p - p_\star^-)$ is the perturbative parameter. However, since $\hat{L}_p{}^{(\mathrm{cH})}$ will generally be nonband diagonal, the order-p representation of QNM radial functions, $|f\rangle$, may not quickly converge to a useful approximation. Unlike approximation with classical polynomials, it is not always possible to reduce error by increasing the order of the confluent Heun polynomial basis used.

These deficits are underpinned by the fact that each order-p confluent Heun polynomial basis is a multiplex, i.e., all members of each confluent Heun polynomial basis are polynomials of the same order. There is, therefore, good reason to wonder if there exists a basis of polynomials, each with a distinct order, that is orthogonal under the scalar product [Eq. (14)].

V. NATURAL AND CANONICAL POLYNOMIALS

The previous discussion does not rule out the *construction* of polynomials that are (*i*) complete in the infinite dimensional sense, (*ii*) orthogonal with respect to the scalar product [Eq. (14)], and (*iii*) can represent $\mathcal{D}_\xi$ as a symmetric matrix. While such polynomials cannot be exactly of the Heun type for the reasons stated in Sec. III, they may yet possess the key features of classical polynomials, namely completeness and orthogonality. In this sense, polynomials with properties (*i*) and (*ii*) will be referred to as *canonical*. Polynomials satisfying (*iii*) will be referred to as *natural* to $\mathcal{D}_\xi$.

For example, the Chebyshev polynomials defined on $\xi \in [0, 1]$ are canonical, but not natural because $\mathcal{D}_\xi$ is not self-adjoint with respect to the Chebyshev inner-product. In contrast, the confluent Heun polynomials discussed in Secs. III and IV are natural to $\mathcal{D}_\xi$, but due to their overcompleteness and atypical orthogonality, they are not canonical.

The possibility that the confluent Heun polynomials may be used to construct polynomials that are *both* natural to $\mathcal{D}_\xi$ and canonical is our present concern. Henceforth, such polynomials will be referred to as *canonical confluent Heun polynomials*. When it is clear that confluent Heun polynomials are being discussed, the canonical confluent Heun polynomials may be simply referred to as the "canonical polynomials."

In this section, two equivalent methods to construct canonical confluent Heun polynomials are described. The first method pertains to the construction of canonical polynomials directly from confluent Heun polynomials defined in Sec. III. This method will be referred to as "*direct construction*." The second method is based upon the standard Gram-Schmidt process. This method will be referred to as "*Gram-Schmidt construction*."

This section concludes with comments on the *equivalence* between direct and Gram-Schmidt construction, their completeness, and finally, two relevant *representations* of the canonical confluent Heun polynomials in terms of the confluent Heun polynomials.

A. Direct construction

Let a canonical confluent Heun polynomial of order p be denoted $|u_p\rangle$, where it is represented in the basis of order p confluent Heun polynomials,

$$|u_p\rangle = \sum_{k=0}^{p} \mathrm{c}_{pk} |y_{pk}\rangle. \tag{40}$$

The direct construction of $|u_p\rangle$ from $|y_{pk}\rangle$ requires the determination of constants, c_{pk}, such that the resulting polynomials are canonical (properties *i* and *ii*), and natural to $\mathcal{D}_\xi$ (property *iii*). We begin our construction with property (*ii*).

Explicitly, property (*ii*) means that

$$\langle u_{p'}|u_p\rangle \propto \delta_{p'p}. \tag{41}$$

We will now show that Eqs. (40) and (41) suffice to determine all expansion coefficients, c_{pk}, via an iterative linear process.

Without loss of generality, let $c_{pp} = 1$. It follows that, for $p = 0$,

$$|u_0\rangle = |y_{00}\rangle. \tag{42}$$

For $p = 1$, applying $c_{11} = 1$ to Eq. (40) means that $|u_1\rangle = c_{10}|y_{10}\rangle + |y_{11}\rangle$. Orthogonality [Eq. (41)] then requires that

$$\langle u_0|u_1\rangle = c_{10}\langle y_{00}|y_{10}\rangle + \langle y_{00}|y_{11}\rangle = 0. \tag{43}$$

Thus, the single unknown constant c_{10} may be solved for, yielding,

$$c_{10} = -\frac{\langle y_{00}|y_{11}\rangle}{\langle y_{00}|y_{10}\rangle}. \tag{44}$$

For $p = 2$, we may again consider $|u_2\rangle$ as defined in Eq. (40), namely $|u_2\rangle = c_{20}|y_{20}\rangle + c_{21}|y_{21}\rangle + |y_{22}\rangle$. Here, c_{20} and c_{21} are the unknowns of interest. Requiring that $\langle u_0|u_2\rangle = 0$ and $\langle u_1|u_2\rangle = 0$ results in two coupled equations,

$$c_{20}\langle u_0|y_{20}\rangle + c_{21}\langle u_0|y_{21}\rangle + \langle u_0|y_{22}\rangle = 0, \tag{45a}$$

$$c_{20}\langle u_1|y_{20}\rangle + c_{21}\langle u_1|y_{21}\rangle + \langle u_1|y_{22}\rangle = 0. \tag{45b}$$

Moving the last terms in Eqs. (45a) and (45b) to their respective right-hand sides yields that

$$c_{20}\langle u_0|y_{20}\rangle + c_{21}\langle u_0|y_{21}\rangle = -\langle u_0|y_{22}\rangle, \tag{46a}$$

$$c_{20}\langle u_1|y_{20}\rangle + c_{21}\langle u_1|y_{21}\rangle = -\langle u_1|y_{22}\rangle. \tag{46b}$$

Equation (46) is equivalent to the linear matrix equation,

$$\hat{X}_2 \vec{c}_2 = \vec{b}_2, \tag{47}$$

where $\hat{X}_2$ has elements $X_{2,jk} = \langle u_j|y_{2k}\rangle$, $\vec{c}_2$ has elements c_{2j}, and $\vec{b}_2$ has elements $b_{2,j} = -\langle u_j|y_{22}\rangle$.

In Eqs. (46) and (47), the essential features of subsequent cases (i.e., $p > 2$) are present: For any $|u_p\rangle$, there will be p equations of the form of Eq. (46), with a total of p unknowns, and this system of linear equations will generally be equivalent to a linear matrix equation,

$$\hat{X}_p \vec{c}_p = \vec{b}_p. \tag{48}$$

As in Eq. (48), $\hat{X}_p$ and $\vec{b}_p$ will generally depend on all polynomials $|u_{p'}\rangle$ with $p' < p$, i.e., all previous iterations. Since both $\{y_{pk}\}_{k=0}^{p}$ and $\{u_{p'}\}_{p'=0}^{p}$ are complete finite dimensional spaces, $\hat{X}_p$ plays the role of a change-of-basis matrix, allowing for the determination of c_{pk} via

$$\vec{c}_p = \hat{X}_p^{-1} \vec{b}_p. \tag{49}$$

In Eq. (49), $\hat{X}_p$ and $\vec{b}_p$ are implicitly functions of all $\vec{c}_{p'}$, where $p' < p$. Thus, given a solution for $\vec{c}_p$, one may then evaluate the right-hand side of Eq. (49) to compute $\vec{c}_{p+1}$ which, in turn, allows for the evaluation of the canonical polynomial, $|u_{p+1}\rangle$ via Eq. (40). In this way, the general determination of canonical confluent Heun polynomials follows inductively from Eqs. (40) and (41).

Having constructed the polynomials, u_p, to be orthogonal, two scaling freedoms remain: signature and normalization. Since the scalar product [Eq. (14)] is unchanged with respect to negation of both of its inputs (e.g., $\langle u_p|u_p\rangle = \langle -u_p|-u_p\rangle$), there is an overall ± 1 scaling, or rather "signature" freedom. Here, this is fixed by dividing each u_p by its value at $\xi = 1$,

$$u_p \leftarrow u_p/u_p(1). \tag{50a}$$

The final freedom is that of normalization. Here, this is fixed in the usual way,

$$u_p \leftarrow u_p/\sqrt{\langle u_p|u_p\rangle}. \tag{50b}$$

B. Gram-Schmidt construction

The well-known Gram-Schmidt process acts on a linearly independent sequence, producing a new sequence that is orthogonal with respect to a chosen scalar product [74]. Given a predefined order for the original sequence, the resulting orthogonal sequence is known to be *unique*, up to normalization choices. In this sense, the familiar classical polynomials (e.g., those of Hermite, Jacobi, and Laguerre) are uniquely defined by applying Gram-Schmidt to the monomials, e.g., ξ^p, such that the resulting polynomial sequence is orthogonal with respect to the relevant inner product [70].

Similarly, the canonical confluent Heun polynomials may be defined by applying Gram-Schmidt to the monomials using the weight function, Eq. (16). Orthogonality is guaranteed because the algorithm iteratively removes the nonorthogonal components between different elements: In particular, given a sequence of monomials $\{\xi^p\}_{p=0}^{\infty}$, the algorithm iteratively defines canonical polynomials, $u_p(\xi)$, to be ξ^p plus a lower-order polynomial that is constrained by requiring that $\langle u_p|u_{p'}\rangle = 0$ for all $p' < p$. The results is a sequence of orthogonal polynomials that can then be normalized according to Eq. (50).

It happens that the weight function used to define the scalar product in Eq. (14) is of the Pollaczek-Jacobi type, but with complex valued parameters [Eqs. (12) and (17)]. Since our weight function may generally be evaluated using analytic continuation see [Eq. (20)], the Gram-Schmidt polynomials described above may be thought of as analytically continued Pollaczek-Jacobi polynomials [73]. Further connections between the polynomials described above, and the Pollaczek-Jacobi polynomials, will be explored in future work [119].

C. Equivalence and completeness

Both direct and Gram-Schmidt constructions of the canonical confluent Heun polynomials are unique iterative processes with identical initial conditions, namely that $|u_0\rangle$ is a constant. In each construction, the requirement of orthogonality, i.e., $\langle u_{p'<p}|u_p\rangle = 0$, uniquely defines $|u_1\rangle$, as well as subsequent polynomials. Since, upon each iteration, there is only one nontrivial result for each $|u_p\rangle$, both processes result in normalized canonical confluent Heun polynomials that are equivalent up to a root-of-unity scaling factor.

Equivalence is easily checked by, e.g., writing $|u_0\rangle$ and $|u_1\rangle$ explicitly as polynomials in ξ, and then verifying that both constructions yield the same result, which is

$$u_0(\xi) = \langle \xi^0\rangle^{-1/2}, \tag{51a}$$

$$u_1(\xi) = \left[\frac{\langle \xi^0\rangle}{\langle \xi^0\rangle\langle \xi^2\rangle - \langle \xi^1\rangle^2}\right]^{1/2}\left(\xi - \frac{\langle \xi^1\rangle}{\langle \xi^0\rangle}\right). \tag{51b}$$

In Eq. (51), we recall that $\langle \xi^k\rangle$ are monomial moments defined by Eq. (20). On arrives at Eqs. (51a) and (51b) regardless of whether direct or Gram-Schmidt construction is used.

Henceforth, we will make no distinction between the canonical confluent Heun polynomials generated by direct or Gram-Schmidt construction.

Regarding completeness, since the results of direct and Gram-Schmidt construction are equivalent, if the result of one construction is complete, then so is the other. The completeness of the Gram-Schmidt constructed polynomials is perhaps the most straightforward. Any sequence of Gram-Schmidt polynomials, if constructed from a complete set, will also be complete. The monomials are complete when all monomial moments are well defined[7] according to Eq. (20) [54,74,120]. For example, in Paper I, it was found that the monomial moments are well defined for all QNM frequencies with nonzero real parts, which is the case for most QNM frequencies of astrophysical relevance. Therefore, we expect that the canonical confluent Heun polynomials will generally be complete in that setting.

Since the confluent Heun polynomials are eigenfunctions to $\mathcal{D}_\xi$, it can be useful to represent each $|u_p\rangle$ in terms of confluent Heun polynomials, $|y_{p'k'}\rangle$. However, since the confluent Heun polynomials are overcomplete, there is no unique representation.

[7]See Sec. VI of Paper I for a detailed discussion.

D. Single and multiorder representations

The overcompleteness of the confluent Heun polynomials means that there are multiple equivalent representations of any integrable function in terms of the confluent Heun polynomials, $|y_{p'k}\rangle$. Here, this fact is applied to the canonical confluent Heun polynomials.

Since each space of order p confluent Heun polynomials is a $p+1$ dimensional basis, the identity operator for all order p polynomials, $\mathbb{I}_p$, may be written as it was in Eq. (26),

$$\mathbb{I}_p = \sum_{k=0}^{p} |y_{pk}\rangle\langle y_{pk}|. \tag{52}$$

Having defined the canonical confluent Heun polynomials, $|u_p\rangle$, two mathematically different but practically equivalent representations result from Eq. (52).

The first is simply the ansatz used for direct construction, i.e., Eq. (40),

$$|u_p\rangle = \mathbb{I}_p|u_p\rangle \tag{53a}$$

$$= \sum_{k=0}^{p} |y_{pk}\rangle\langle y_{pk}|u_p\rangle \tag{53b}$$

$$= \sum_{k=0}^{p} c_{pk}|y_{pk}\rangle. \tag{53c}$$

In Eqs. (53a) and (53b), the order-p identity operator, $\mathbb{I}_p$, has been applied to $|u_p\rangle$. In Eq. (53c), it is noted that $c_{pk} = \langle y_{pk}|u_p\rangle$. The direct construction algorithm discussed previously is simply a way to determine $\langle y_{pk}|u_p\rangle$ when $|u_p\rangle$ is unknown.

Within Eq. (53), each canonical confluent Heun polynomial is represented in the basis of a different polynomial order, meaning that a set of multiple canonical confluent Heun polynomials would require the generation of confluent Heun polynomials from multiple orders. This is evident in Eq. (53) by $|u_p\rangle$ on the left-hand side having the same label, p, as the upper limit of the sum on the right-hand side. Thus, for each different polynomial order, a different confluent Heun polynomial basis is considered. For this reason, Eq. (53) will henceforth be referred to as the *multiorder representation* of the canonical confluent Heun polynomials.

For any finite sequences of canonical confluent Heun polynomials, $\{|u_p\rangle\}_{p=0}^{p'}$, the multiorder representation requires the evaluation of all polynomials within the set $\cup_{p=0}^{p'} \{|y_{pk}\rangle\}_{k=0}^{p}$. Since there will be $\frac{1}{2}(p'+1)(p'+2)$ such polynomials, their evaluation presents a significant, but ultimately avoidable, computational expense.

A second representation allowed by Eq. (52) entails choosing a single confluent Heun polynomial basis of order p' to represent all canonical confluent Heun polynomials with $p \le p'$,

$$|u_p\rangle = \mathbb{I}_{p'}|u_p\rangle \tag{54a}$$

$$= \sum_{k=0}^{p'} |y_{p'k}\rangle\langle y_{p'k}|u_p\rangle \tag{54b}$$

$$= \sum_{k=0}^{p'} d_{p'pk}|y_{p'k}\rangle. \tag{54c}$$

We emphasize that, unlike Eq. (53), $|u_p\rangle$ in the left-hand side of Eq. (54) has a label p that differs from the upper limit in the sum on the right-hand side of Eq. (54). In Eqs. (54a) and (54b), the identity operator for the order-p' confluent Heun polynomials has been applied to $|u_p\rangle$ and in Eq. (54c),

$$d_{p'pk} = \langle y_{p'k}|u_p\rangle. \tag{55}$$

In practice, one may first generate $|u_p\rangle$ via Gram-Schmidt construction, and then explicitly compute $\langle y_{p'k}|u_p\rangle$ using Eq. (19). Equation (54) will henceforth be referred to as the *single-order representation* of the canonical confluent Heun polynomials. If the largest polynomial order of interest is p', then the single-order representation has the practical advantage of only requiring $p'+1$ confluent Heun polynomials to be computed after Gram-Schmidt construction.

VI. TRIDIAGONALIZATION

We may now return to Teukolsky's radial equation for QNMs,

$$\mathcal{L}_\xi|f\rangle = A|f\rangle. \tag{56}$$

Having determined canonical polynomials that are natural to $\mathcal{L}_\xi$, their completeness and orthogonality may be used to represent Eq. (56) as a simple linear matrix equation.

Since the canonical confluent Heun polynomials are complete, we may use them to represent the identity operator,

$$\mathbb{I} = \sum_{p=0}^{\infty} |u_p\rangle\langle u_p|. \tag{57}$$

This allows each operator and vector within Eq. (56) to be projected into the basis of canonical confluent Heun polynomials,

$$\mathbb{I}\mathcal{L}_\xi\mathbb{I}|f\rangle = A\mathbb{I}|f\rangle. \tag{58}$$

Using Eq. (57) to expand Eq. (58) yields

$$\sum_{p,q} |u_p\rangle\langle u_p|\mathcal{L}_\xi|u_q\rangle\langle u_q|f\rangle = A\sum_p |u_p\rangle\langle u_p|f\rangle, \tag{59a}$$

$$\hat{L}\vec{f} = A\vec{f}. \tag{59b}$$

In going from Eqs. (59a) to (59b), we recognize $\hat{L}$ to be the matrix whose elements are

$$L_{pq} = \langle u_p|\mathcal{L}_\xi|u_q\rangle, \tag{60}$$

and $\vec{f}$ to be the vector whose elements are

$$f_p = \langle u_p|f\rangle. \tag{61}$$

Recall that since $\mathcal{L}_\xi$ is self-adjoint with respect to the scalar product, the following equivalences hold: $\langle u_p|\mathcal{L}_\xi|u_q\rangle = \langle u_p|\mathcal{L}_\xi u_q\rangle = \langle \mathcal{L}_\xi u_p|u_q\rangle$.

In this section, two mathematically different but practically equivalent routes to tridiagonalizing $\hat{L}$ are presented. The first route is based upon the single-order representation of the canonical confluent Heun polynomials, and it will be discussed in detail. The second route is based upon their multiorder representation, and it will be described summarily as the step-by-step reasoning is both similar to that of the single-order approach, and already detailed in Paper I.

Regardless of the representation used, the result is the same: the confluent Heun operator $\mathcal{L}_\xi$ is approximated by a matrix, $\hat{L}$ that is of finite size, symmetric, and tridiagonal. In effect, the complex Jacobi matrix of $\mathcal{L}_\xi$ is determined [80,81].

Our present concern is the structure of $\hat{L}$. Since its matrix elements are $\langle u_p|\mathcal{L}_\xi u_q\rangle$, the action of $\mathcal{L}_\xi$ on $|u_q\rangle$ must first be understood,

$$\mathcal{L}_\xi|u_q\rangle = (\mathrm{C}_0 + \mathrm{C}_1[1-\xi])|u_q\rangle \tag{62a}$$

$$+\mathcal{D}_\xi|u_q\rangle. \tag{62b}$$

In Eq. (62), as in Eq. (11), $\mathcal{L}_\xi$ has been written in terms of the physical constants C_0 and C_1 [Eq. (62a)], as well as the confluent Heun operator $\mathcal{D}_\xi$ [Eq. (62b)]. Plainly, Eq. (62a) only contains constant rescalings of $|u_p\rangle$ and terms dependent on $\xi|u_q\rangle$, and Eq. (62b) is simply $\mathcal{D}_\xi|u_q\rangle$. Since $\langle u_p|u_q\rangle = \delta_{pq}$, constant rescalings of $|u_p\rangle$ will only contribute to the diagonal of $\hat{L}$. Therefore, to understand the structure of $\hat{L}$, we must first refine our understanding of $\xi|u_q\rangle$ and $\mathcal{D}_\xi|u_q\rangle$.

It happens that $\xi|u_q\rangle$ can be represented in terms of only three canonical polynomials,

$$\xi|u_q\rangle = \sigma_{q0}|u_{q-1}\rangle + \sigma_{q1}|u_q\rangle + \sigma_{q2}|u_{q+1}\rangle. \tag{63}$$

Equation (63) is a three-term recursion relationship between canonical confluent Heun polynomials. It is a standard result in polynomial theory and can be understood as resulting from completeness, orthogonality, and symmetry of the scalar product, namely $\langle u_p|\xi u_q\rangle = \langle \xi u_p|u_q\rangle$.

In Eq. (63), the recursion coefficients, σ_{q0}, σ_{q1}, and σ_{q2} are p-dependent complex numbers. Unlike many instances in polynomial theory where the recursion coefficients are known analytically, here they are to be treated numerically, as determined by evaluation of the scalar product:

$$\sigma_{q0} = \langle u_{q-1}|\xi u_q\rangle, \tag{64a}$$

$$\sigma_{q1} = \langle u_q|\xi u_q\rangle, \tag{64b}$$

$$\sigma_{q2} = \langle u_{q+1}|\xi u_q\rangle. \tag{64c}$$

In the context of $\mathcal{L}_\xi|u_q\rangle$ [i.e., [Eq. (62)], the existence of a three-term recursion relationship between polynomials means that terms within Eq. (62a) only contribute to the central, lower, and upper diagonal of $\hat{L}$. Therefore, Eq. (62a) will generally contribute to the tridiagonal part of $\hat{L}$.

This should be expected of Eq. (62a) since all canonical type polynomials (e.g., Chebyshev and Laguerre) have three-term recursions. However, since not all canonical polynomials are natural to $\mathcal{D}_\xi$, it happens that $\mathcal{D}_\xi|u_q\rangle$ is a problem-specific quantity.

Further, since $\mathcal{D}_\xi$ contains derivatives, it is here that the representation of each $|u_q\rangle$ has meaningful effect: while the previously discussed single- and multiorder representations are equivalent Eqs. (53) and (54)], their behaviors under differentiation are not.

A. The single-order approach

We may first consider the single-order representation of the canonical confluent Heun polynomials. In that picture, any polynomial of order q is expanded in terms of confluent Heun polynomials of order $p' \geq q$ [Eq. (56)]. For a canonical confluent Heun polynomial $|u_q\rangle$, this expansion is written as

$$|u_q\rangle = \sum_{k=0}^{p'} d_{p'qk}|y_{p'k}\rangle. \tag{65}$$

Therefore, the action of $\mathcal{D}_\xi$ on $|u_q\rangle$ is given by

$$\mathcal{D}_\xi|u_q\rangle = \sum_{k=0}^{p'} d_{p'qk}\mathcal{D}_\xi|y_{p'k}\rangle \tag{66a}$$

$$= \sum_{k=0}^{p'} d_{p'qk}(\lambda_{p'k} + \mu_{p'}\xi)|y_{p'k}\rangle, \tag{66b}$$

$$= |v_{p'q}\rangle + \mu_{p'}\xi|u_q\rangle. \tag{66c}$$

In Eq. (66b), the two parameter eigenvalue relation for the confluent Heun polynomials, Eq. (22a), has been applied. In Eq. (66c), terms that depend on $\lambda_{p'k}$ have been grouped to define a new polynomial,

$$|v_{p'q}\rangle = \sum_{k=0}^{p'} d_{p'qk}\lambda_{p'k}|y_{p'k}\rangle, \tag{67}$$

and it has been noticed that remaining terms in Eq. (66) are simply proportional to $|u_q\rangle$. Since $\mathcal{D}_\xi$ increases the order of polynomials by one (see Sec. III), $|v_{p'q}\rangle$ has order $q+1$.

It follows [from Eqs. (62) and (66c)] that $\mathcal{L}_\xi|u_q\rangle$ may be written as

$$\mathcal{L}_\xi|u_q\rangle = (\mathrm{C}_0 + \mathrm{C}_1)|u_q\rangle \tag{68a}$$

$$+ |v_{p'q}\rangle \tag{68b}$$

$$+ \alpha_{p'}\xi|u_q\rangle. \tag{68c}$$

In Eq. (68c), recall that $\alpha_{p'}$ is defined in Eq. (36). The structure of Eq. (68) enables a few useful observations. Equations (68a)–(68c) imply that $\hat{L}$ is the sum of three matrices, $\hat{L}_0^{(\mathrm{S})}$, $\hat{L}_1^{(\mathrm{S})}$, and $\hat{L}_2^{(\mathrm{S})}$,

$$\hat{L} = \hat{L}_0^{(\mathrm{S})} + \hat{L}_1^{(\mathrm{S})} + \hat{L}_2^{(\mathrm{S})}. \tag{69}$$

Their respective matrix elements are

$$L_{0,pq}^{(\mathrm{S})} = (\mathrm{C}_0 + \mathrm{C}_1)\delta_{pq}, \tag{70a}$$

$$L_{1,pq}^{(\mathrm{S})} = \langle u_p|v_{p'q}\rangle, \tag{70b}$$

$$L_{2,pq}^{(\mathrm{S})} = \alpha_{p'}\langle u_p|\xi u_q\rangle. \tag{70c}$$

Since $\mathcal{L}_\xi$ is self-adjoint with respect to the scalar product, $\hat{L}$ will be symmetric, meaning that $L_{pq} = L_{qp}$. It may be observed that $\hat{L}_0^{(\mathrm{S})}$ and $\hat{L}_2^{(\mathrm{S})}$ are symmetric, owing to the symmetry of the Kronecker delta and of the scalar product. Thus for $\hat{L}_0^{(\mathrm{S})} + \hat{L}_1^{(\mathrm{S})} + \hat{L}_2^{(\mathrm{S})}$ to be symmetric, $\hat{L}_1^{(\mathrm{S})}$ must be symmetric, meaning that

$$\langle u_p|v_{p'q}\rangle = \langle v_{p'p}|u_q\rangle. \tag{71}$$

This conclusion may also be reached via the consideration of $\langle u_p|\mathcal{D}_\xi u_q\rangle = \langle \mathcal{D}_\xi u_p|u_q\rangle$, which directly reduces to Eq. (71). Thus, Eq. (71) is only true for scalar products under which $\mathcal{D}_\xi$ is self-adjoint (e.g., [Eq. (71)] does not hold for Chebyshev inner-product, meaning that the associated $\hat{L}_1^{(\mathrm{S})}$ matrix would not be symmetric) [54].

Lastly, it may be deduced that $\hat{L}_1^{(\mathrm{S})}$ is tridiagonal. This follows from the fact that each $|v_{p'q}\rangle$ is of order $q+1$. In particular, given any order $q+1$ polynomial, e.g., $|v_{p'q}\rangle$, its canonical confluent Heun polynomial representation will not contain contributions from $|u_p\rangle$ if $p > q+1$,

$$|v_{p'q}\rangle = \mathbb{I}|v_{p'q}\rangle \tag{72a}$$

$$= \sum_{p=0}^{\infty} |u_p\rangle\langle u_p|v_{p'q}\rangle, \tag{72b}$$

$$= \sum_{p=0}^{q+1} |u_p\rangle\langle u_p|v_{p'q}\rangle. \tag{72c}$$

In Eqs. (72a)–(72b), a canonical confluent Heun polynomial representation is applied to $|v_{p'q}\rangle$. In Eq. (72c), it has been acknowledged that terms with $p > q+1$ do not contribute; otherwise, the resulting polynomial would be of order greater than $q+1$. This condition on $\langle u_p|v_{p'q}\rangle$, as well as its counterpart on $\langle u_q|v_{p'p}\rangle$, may be stated thusly,

$$\langle u_p|v_{p'q}\rangle = 0, \quad \text{if } p > q+1, \tag{73a}$$

$$\langle u_q|v_{p'p}\rangle = 0, \quad \text{if } q > p+1. \tag{73b}$$

Note that $\langle u_q|v_{p'p}\rangle = \langle v_{p'p}|u_q\rangle$, not due to Eq. (71), but rather to the multiplicative associative property applied to the integrand of the scalar product [Eq. (14)]. Also note that the conditional in Eq. (73) is equivalent to $p < q-1$.

Since Eqs. (73a) and (73b) hold simultaneously, it follows that $\langle u_p|v_{p'q}\rangle \neq 0$ when $q-1 \leq p \leq q+1$. In other words, each $|v_{p'q}\rangle$ is exactly equal to a sum over only three canonical confluent Heun polynomials,

$$|v_{p'q}\rangle = \nu_{q0}|u_{q-1}\rangle + \nu_{q1}|u_q\rangle + \nu_{q2}|u_{q+1}\rangle. \tag{74}$$

In Eq. (74), ν_{q0}, ν_{q1}, and ν_{q2} are complex valued q-dependent numbers defined by the scalar product,

$$\nu_{q0} = \langle u_{q-1}|v_{p'q}\rangle, \tag{75a}$$

$$\nu_{q1} = \langle u_q|v_{p'q}\rangle, \tag{75b}$$

$$\nu_{q2} = \langle u_{q+1}|v_{p'q}\rangle. \tag{75c}$$

The elements of $\hat{L}_1^{(\mathrm{S})}$, namely $\langle u_p|v_{p'q}\rangle$, are only nonzero between its upper and lower diagonal, so $\hat{L}_1^{(\mathrm{S})}$ is a tridiagonal matrix.

Since $\hat{L}_1^{(\mathrm{S})}$ and $\hat{L}_2^{(\mathrm{S})}$ are symmetric and tridiagonal, and $\hat{L}_0^{(\mathrm{S})}$ is diagonal, if follows that $\hat{L} = \hat{L}_0^{(\mathrm{S})} + \hat{L}_1^{(\mathrm{S})} + \hat{L}_2^{(\mathrm{S})}$ is symmetric and tridiagonal. Equivalently,

$$\mathcal{L}_\xi|u_q\rangle = \nu_{q3}|u_{q-1}\rangle + \nu_{q4}|u_q\rangle + \nu_{q5}|u_{q+1}\rangle, \tag{76}$$

where

$$\nu_{q3} = \alpha_{p'}\sigma_{q0} + \nu_{q0}, \tag{77a}$$

$$\nu_{q4} = \alpha_{p'}\sigma_{q1} + \nu_{q1} + (\mathrm{C}_0 + \mathrm{C}_1), \tag{77b}$$

$$\nu_{q5} = \alpha_{p'}\sigma_{q2} + \nu_{q2}. \tag{77c}$$

In Eq. (77), we recall from Eq. (36) that $\alpha_{p'} = \mu_{p'} - \mathrm{C}_1$, and that σ_{q0}, σ_{q1}, and σ_{q2} are defined by Eq. (64).

B. The multiorder approach

Here, an alternative approach to tridiagonalization is summarized, following and building upon Sec. VIII of Paper I. This approach uses the multiorder representation of the canonical confluent Heun polynomials,

$$|u_q\rangle = \sum_{k=0}^{q} c_{qk}|y_{qk}\rangle. \tag{78}$$

While the net result, namely $\hat{L}$, is the same as that found previously, the multiorder approach enables the derivation of relationships between $\hat{L}$ and the canonical confluent Heun polynomials' three-term recursion that are ostensibly hidden within the single-order approach. This point is illustrated by first applying the multiorder representation of the canonical confluent Heun polynomials to the radial problem and then using the symmetry of the Jacobi matrix $\hat{L}$ to relate elements of $\hat{L}$ to the canonical confluent Heun polynomials' three-term recursion. This proceeds as follows.

Under the multiorder approach, $\hat{L}$ may be written as the sum of three matrices,

$$\hat{L} = \hat{L}_0^{(\mathrm{M})} + \hat{L}_1^{(\mathrm{M})} + \hat{L}_2^{(\mathrm{M})}. \tag{79}$$

Their respective matrix elements are

$$L_{0,pq}^{(\mathrm{M})} = (\mathrm{C}_0 + \mathrm{C}_1)\delta_{pq}, \tag{80a}$$

$$L_{1,pq}^{(\mathrm{M})} = \langle u_p|v_q\rangle, \tag{80b}$$

$$L_{2,pq}^{(\mathrm{M})} = \alpha_q\langle u_p|\xi u_q\rangle. \tag{80c}$$

In Eq. (80), $|v_q\rangle$ is an order-q "auxiliary" polynomial defined as

$$|v_q\rangle = \sum_{k=0}^{q} \mathrm{c}_{qk}\lambda_{qk}|y_{qk}\rangle, \tag{81}$$

where it is recalled that λ_{qk} is the eigenvalue of the confluent Heun polynomial, $|y_{qk}\rangle$. Consideration of $\langle u_p|\mathcal{D}_\xi u_q\rangle = \langle \mathcal{D}_\xi u_p|u_q\rangle$ yields that $|v_q\rangle$ may be equated with a sum over only a few canonical confluent Heun polynomials,

$$|v_q\rangle = \sigma_{q3}|u_{q-1}\rangle + \sigma_{q4}|u_q\rangle. \tag{82}$$

In Eq. (82), σ_{q3} and σ_{q4} are complex valued q-dependent numbers defined by the scalar product,

$$\sigma_{q3} = \langle u_{q-1}|v_q\rangle, \tag{83a}$$

$$\sigma_{q4} = \langle u_q|v_q\rangle. \tag{83b}$$

It may be observed that $\hat{L}_0^{(\mathrm{M})}$ is diagonal, $\hat{L}_1^{(\mathrm{M})}$ upper-tridiagonal due to [Eq. (82)], and $\hat{L}_2^{(\mathrm{M})}$ is tridiagonal. Therefore, $\hat{L}$ is tridiagonal as expected.

It is informative to note that, while $\hat{L}_0^{(\mathrm{M})}$ is symmetric, Eqs. (80b) and (80c) are *asymmetric*: Eq. (80b) is asymmetric due to Eq. (82) not having a contribution from $|u_{q+1}\rangle$ (i.e., $\hat{L}_1^{(\mathrm{M})}$ is only upper-tridiagonal), and Eq. (80c) is asymmetric due to the q-dependent scale factor, α_q. Thus, since $\hat{L}$ is symmetric, $\hat{L}_1^{(\mathrm{M})}$ and $\hat{L}_2^{(\mathrm{M})}$ must combine to form a quantity that is also symmetric. In turn, this means that $\hat{L}_1^{(\mathrm{M})}$ and $\hat{L}_2^{(\mathrm{M})}$ are not independent objects.

The link between $\hat{L}_1^{(\mathrm{M})}$ and $\hat{L}_2^{(\mathrm{M})}$ is perhaps easiest to understand by noting that the multiorder representation of the canonical confluent Heun polynomials allows $\mathcal{L}_\xi|u_q\rangle$ to be written as

$$\mathcal{L}_\xi|u_q\rangle = \sigma_{q5}|u_{q-1}\rangle + \sigma_{q6}|u_q\rangle + \sigma_{q7}|u_{q+1}\rangle, \tag{84}$$

where

$$\sigma_{q5} = \alpha_q\sigma_{q0} + \sigma_{q3}, \tag{85a}$$

$$\sigma_{q6} = \alpha_q\sigma_{q1} + \sigma_{q4} + (\mathrm{C}_0 + \mathrm{C}_1), \tag{85b}$$

$$\sigma_{q7} = \alpha_q\sigma_{q2}. \tag{85c}$$

Plainly stated, since $\hat{L}$ is a symmetric matrix its matrix elements, L_{pq}, are such that $L_{pq} = L_{qp}$. Equation (85) means that L_{pq} will be within the set $\{\sigma_{q5}, \sigma_{q6}, \sigma_{q7}\}$ for $p \in \{q-1, q, q+1\}$, respectively. Since $\hat{L}$ is tridiagonal, the only nontrivial symmetry statement is $L_{q-1,q} = L_{q,q-1}$, which is equivalent to $L_{q,q+1} = L_{q+1,q}$ under $q \to q+1$. Using equation Eqs. (84) and (85), $L_{q-1,q} = L_{q,q-1}$ becomes

$$\sigma_{q5} = \sigma_{q-1,7}, \tag{86a}$$

$$\alpha_q\sigma_{q0} + \sigma_{q3} = \alpha_{q-1}\sigma_{q-1,2}. \tag{86b}$$

In Eq. (86a), $L_{q-1,q} = L_{q,q-1}$ has been rewritten using Eq. (84). In going from Eqs. (86a) to (86b), (85) has been used to expand both sides. Equation (86b) may be further reduced by noting that symmetry of the canonical polynomials' three-term recursion [see [Eq. (63)]] means that $\sigma_{q-1,2} = \sigma_{q0}$. Therefore, Eq. (86b) allows σ_{q3} (i.e., $\langle u_{q-1}|v_q\rangle$) to be written as

$$\sigma_{q3} = (\alpha_{q-1} - \alpha_q)\sigma_{q0}, \tag{87a}$$

$$\langle u_{q-1}|v_q\rangle = (2(q-1) + \mathrm{C}_4)\langle u_{q-1}|\xi u_q\rangle. \tag{87b}$$

In Eqs. (87a), (86b) as been solved for σ_{q3}. In Eq. (87b), σ_{q3} and σ_{q0} have been replaced with their scalar-product definitions via Eqs. (62a), (83a), (22b), and (27) have been used to rewrite instances of α_q.

Equation (87b) communicates that the nonzero off-diagonal elements of $\hat{L}_1^{(\mathrm{M})}$, namely $\langle u_{q-1}|v_q\rangle$, are directly proportional to the three-term recursion coefficient, $\langle u_{q-1}|\xi u_q\rangle$. Recalling Eq. (80c), the same is clearly true for off-diagonal elements of $\hat{L}_2^{(\mathrm{M})}$. Together, those two observations mean that the off-diagonal elements of $\hat{L}$ are generally proportional to the three-term recursion coefficients σ_{q0} and σ_{q2}.

VII. SELECT NUMERICAL RESULTS

Before being put into practice, the preceding theoretical development benefits from a few points of guidance [54]. For all computations, physical parameters, namely $\{a/M, s, \tilde{\omega}, m\}$, must be chosen such that the derived parameters, C_1 through C_4, may then be computed according to Eq. (12). For nearly all subsequent manipulations involving polynomials or series expansions, the fundamental operation is the scalar product [see [Eq. (14)]].

While it is possible to evaluate the scalar product by directly integrating it, success in that endeavor requires the formulation of a complex path that avoids singularities in the integrand [54]. A much simpler method of evaluating the scalar product is given by Eqs. (19) and (20), which reduces the effort to the evaluation of standard special functions via their well-known analytic continuations.

Given the scalar product, it is subsequently useful to determine the eigenvectors and values of matrices, such as $\hat{L}$ which encodes the QNM problem [Eq. (59b)]. This may be accomplished with any of several standard linear algebra packages [121,122]. Henceforth, Eq. (19) is used to compute all scalar product, and Eq. (20) is implemented with 128 decimal points of general precision arithmetic via the Python package, MPMATH [122]. This package is also used to solve various matrix eigenvalue problems.

In this section, example applications of the canonical confluent Heun polynomials are provided along with related practical guidance. While many cases are considered, most examples are connected by a single fiducial case: a Kerr BH of dimensionless spin $a/M = 0.7$ and its QNM with $(s, \ell, m, n) = (-2, 2, 2, 6)$. Broadly, examples range from the brief consideration of the canonical confluent Heun polynomials to their application to the confluent Heun polynomial and QNM problems. In the latter example, the QNMs' radial functions are explicitly computed and shown to satisfy Teukolsky's radial equation [Eq. (13)]. This section concludes with a brief discussion of the transition from Schwarzschild to Kerr, from the perspective of the QNM radial functions.

A. Canonical confluent Heun polynomials

Examples of the first five canonical confluent Heun polynomials are shown in Fig. 2.

As seen in the top panel of Fig. 2, the polynomials may be formatted such that their real parts have zero roots along the real line, meaning that the net complex valued polynomials will have no roots at real values of the fractional radial coordinate, ξ. This is simply a result of the fact that the canonical confluent Heun polynomials have complex

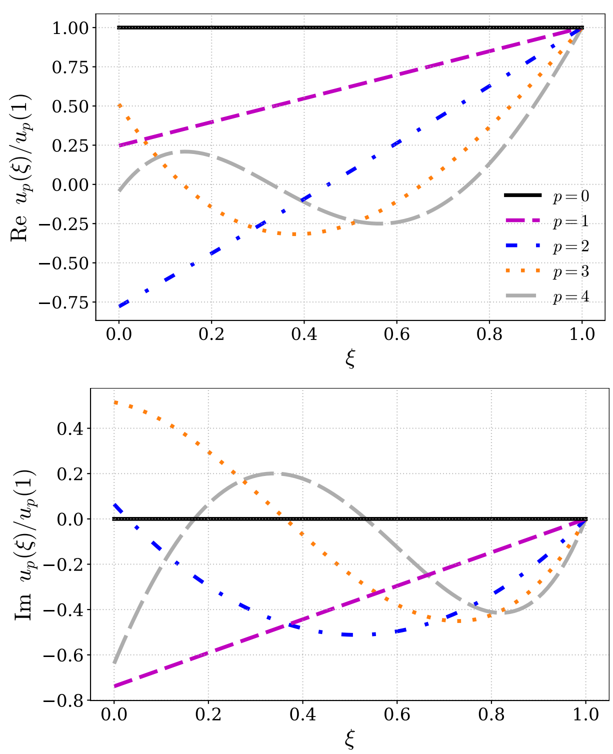

FIG. 2. The first five canonical confluent Heun polynomials, i.e., $u_p(\xi)$ with $p \in \{0, 1, 2, 3, 4\}$. Polynomials are constructed using field spin weight $s = -2$, BH spin $a/M = 0.7$, and Kerr QNM frequency $M\tilde{\omega}_{220} = 0.5326 - 0.0808i$. For ease of presentation, polynomials have been divided by their value at $\xi = 1$ (i.e., spatial infinity). Top panel: real part of each polynomial. Bottom panel: imaginary part of each polynomial. Related discussion is provided in Sec. VII.

valued coefficients [Eq. (51)] and so will generally have roots situated away from the real line.

B. Tridiagonalization

The canonical confluent Heun polynomials may be used to tridiagonalize confluent Heun equations such as the QNM's radial equation [Eq. (13)] or the confluent Heun polynomial equation [Eq. (22)].

In Fig. 3 a step-by-step application of the canonical confluent Heun polynomials to the QNM radial problem is shown. There, the top three panels [i.e., (a), (c), and (e)] show quantities derived directly from the canonical confluent Heun polynomials. The remaining panels show how the multiorder representation [Eq. (78)] of each quantity contributes to the representation of the radial differential operator according to Eq. (79).

When written in terms of matrix elements, Eq. (79) is

$$L_{pq} = L^{(\mathrm{M})}_{0,pq} + L^{(\mathrm{M})}_{1,pq} + L^{(\mathrm{M})}_{2,pq}. \tag{88}$$

Under this framing, the qualitative features of panels (b), (d), and (f) are determined by those of panels (a), (c), and (e), respectively.

Conceptually, canonical confluent Heun polynomial orthogonality [Eq. (41)] is demonstrated in panel (a), upper tridiagonality of auxiliary polynomials [Eq. (82)] is demonstrated in panel (c), and three-term recursion [Eq. (64)] is demonstrated in panel (e). Then end result, panel (g), may be considered to represent the three-term recursion of orthogonal polynomials which approximate solutions to the QNM radial problem [80,81].

1. Matrix asymptotics and truncation

Even if the operator $\mathcal{L}_\xi$ is self-adjoint with respect to a given scalar product, this does not guarantee that its matrix representation will have eigenvalues that accurately approximate those of $\mathcal{L}_\xi$. The extent of agreement between the two sets of eigenvalues depends on the asymptotic behavior of the matrix's off-diagonal elements [96]. By asymptotic, we refer to the behavior of matrix elements L_{pq} with $q \in \{p-1, p, p+1\}$, as p tends towards infinity.

For example, it is well known that the spherical harmonics are an excellent basis in which to represent the QNMs' spheroidal harmonics [13,41,55,56,93]. In part, this is because, when represented in a spherical harmonic basis, the spheroidal harmonic differential operator is asymptotically diagonal,[8] meaning that large-ℓ spheroidal harmonics are asymptotically equivalent spherical harmonics of the same ℓ [41,55,56]. As a result, one can typically estimate spheroidal harmonic eigenvalues with little concern for truncation error by first casting the problem into a spherical harmonic basis and then solving the corresponding matrix eigenvalue problem [41,55,56,93].

We now discuss why this is typically not the case for the QNMs' radial problem. In short, off-diagonal matrix elements for the radial problem typically grow *at least as fast* as the diagonal ones, meaning that the matrix does not become asymptotically diagonal. This behavior is explicit in the radial functions' Frobenius-type series solution, as studied by Refs. [15,39,41,43], and is therefore necessarily present in any orthonormal polynomial representation of the same problem[9] [77,85,124]. In effect, the slow convergence of the radial functions' series solutions, along with truncation thereof, results in what is known as *spectral pollution* [97–100].

For the canonical confluent Heun polynomials, panel (e) of Fig. 3 illustrates a general observation, namely that the large-p structure of three-term recursion is that of a tridiagonal Toeplitz matrix (i.e., a symmetric matrix with constant elements along its diagonals). It follows from the role of $\alpha_p = (p - p^+_\star)(p - p^-_\star)$ in Eq. (85) that all L_{pq} (with $q \in \{p-1, p, p+1\}$) are asymptotically equivalent to p^2. Therefore, the matrix representation of the radial operator is not asymptotically diagonal and not self-adjoint in the sense defined in Ref. [96]. The related qualitative behavior is seen in panel (g) of Fig. 3, which shows matrix elements having a local minimum near $p = q = 6$, before becoming increasingly comparable as p and q increase.

In forthcoming numerical results, we show both the eigenvalues that result from spectral pollution, as well as those consistent with the nontruncated (infinite dimensional) eigenvalue problem. In the latter case, eigenvalues were determined by using an $N = 60$ dimensional canonical confluent Heun polynomial basis, and then truncation-induced eigenvectors were removed. Consistency with the nontruncated problem was checked by comparing against the continued-fraction result[10] [15,39].

C. Polynomial/nonpolynomial duality

The canonical confluent Heun polynomials, $|u_p\rangle$, may be applied to the confluent Heun polynomial problem. In doing so, a quantitative example of polynomial/nonpolynomial duality is encountered, along with related insights into the QNM problem.

[8]This can be seen computing the spherical-spheroidal mixing coefficients and then considering the limit as $\ell \to \infty$ [56,94].

[9]This is due to the fact that the three-term recursions for the series solution must be asymptotically equivalent to the effective tridiagonalization of any polynomial representation. While many polynomial representations will not result in tridiagonal operators, all such operators can be numerically tridiagonalized using standard techniques [123].

[10]The continued-fraction result is also prone to spectral pollution. However, it can typically be avoided in that context, if $\mathcal{O}(10^4)$ terms are considered in the series solution [39,41].

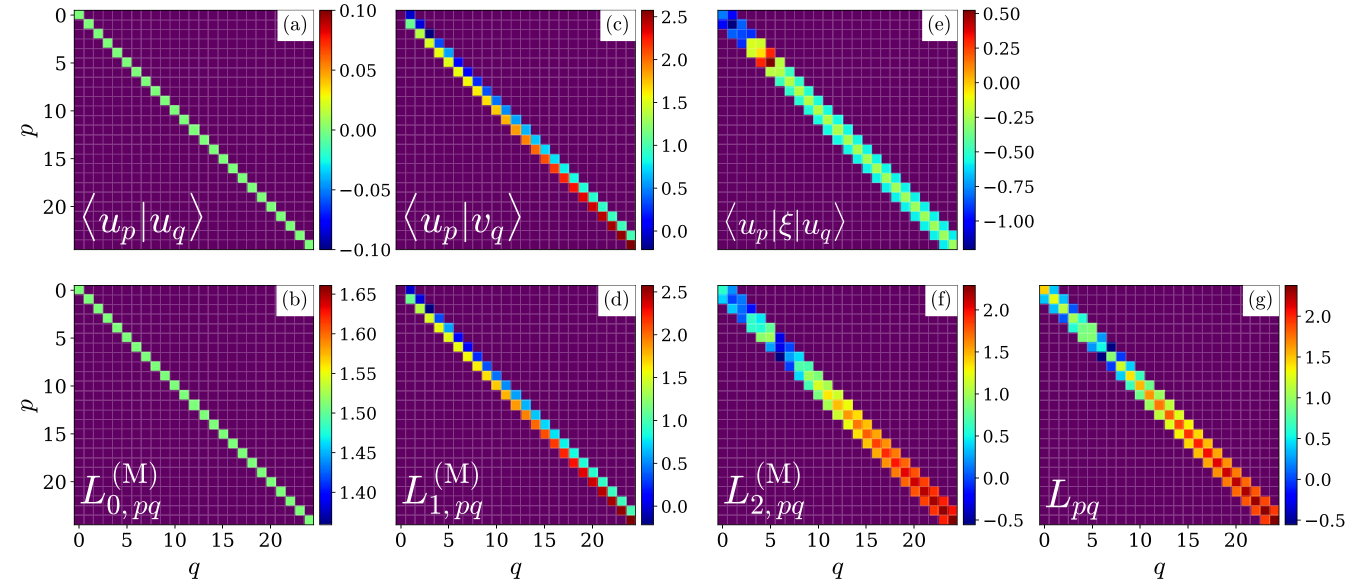

FIG. 3. Matrices related to canonical confluent Heun polynomials and representations of Teukolsky's radial operator for $(s, \ell, m, n) = (-2, 2, 2, 6)$, $a/M = 0.7$, and $M\tilde{\omega}_{\ell mn} = 0.4239 - 1.0954i$. All color bars correspond to the $\log_{10}$ of the absolute values of quantities noted in annotation, e.g., for panel (a), $\log_{10}|\langle u_p|u_q\rangle|$ is visualized. Tiles (in purple) away from each panel's tridiagonal band are exactly zero. See Sec. VII for related discussion.

The confluent Heun polynomial problem was stated in Eq. (22) as

$$\mathcal{D}_\xi|y_{pk}\rangle = (\lambda_{pk} + \mu_p\xi)|y_{pk}\rangle. \tag{89a}$$

To apply the canonical confluent Heun polynomials, Eq. (89) may be restated as

$$\mathcal{L}^{(p)}_\xi|y_{pk}\rangle = \lambda_{pk}|y_{pk}\rangle, \tag{89b}$$

where

$$\mathcal{L}^{(p)}_\xi = -\mu_p\xi + \mathcal{D}_\xi. \tag{89c}$$

By using the canonical confluent Heun polynomials, Eq. (89b) may be rewritten as

$$\hat{L}^{(p)}\vec{y}_{pk} = \lambda_{pk}\vec{y}_{pk}, \tag{90}$$

where $\hat{L}^{(p)}$ and $\vec{y}_{pk}$, respectively, have elements given by

$$L^{(p)}_{\alpha\beta} = \langle u_\alpha|\mathcal{L}^{(p)}_\xi|u_\beta\rangle, \tag{91a}$$

$$y_{pk,\beta} = \langle u_\beta|y_{pk}\rangle. \tag{91b}$$

Since k and α are both integers between 0 and p, the sequence of all eigenvectors comprise the rows of a matrix whose elements are $y_{p\alpha,\beta}$. Similarly, the eigenvalues may be labeled as $\lambda_{p\alpha}$ rather than λ_{pk}.

At focus in Fig. 4 are the confluent Heun polynomial problem's matrix representation, eigenvectors, and eigenvalues for order-6 polynomials. Physical parameters used are identical to those in Table I for $(\ell, m, n) = (2, 2, 6)$.

In panel (a) of Fig. 4, $L^{(p)}_{\alpha\beta}$ are shown. There it may be observed that

$$L^{(p)}_{6,7} = L^{(p)}_{7,6} = 0. \tag{92}$$

This is consistent with the so-called "Δ_{p+1} condition," which is used to define the confluent Heun polynomials via a finite dimensional matrix eigenvalue problem (see Eq. (79) of Paper I as well as Refs. [41,58]). There, the basic concept is that a power series solution to Eq. (89b) will terminate after $p+1$ terms if the Δ_{p+1} condition on a related three-term recursion is satisfied.

The Δ_{p+1} condition is unable to provide insight on the nonpolynomial solutions, simply due to fact that these solutions have series expansions of infinite length. In other words, the nonpolynomial solutions satisfy an infinite dimensional matrix eigenvalue problem, rather than a finite dimensional one.[11] Unlike the power-series perspective of the Δ_{p+1} condition, the canonical confluent Heun polynomial representation of the problem naturally applies to finite and infinite dimensional problems: i.e., the

[11]In such cases, standard routes to finding solutions include the use of continued fractions (see, e.g., Ref. [15]) or the representation of the problem with an orthonormal basis, such as the canonical confluent Heun polynomial basis introduced here.

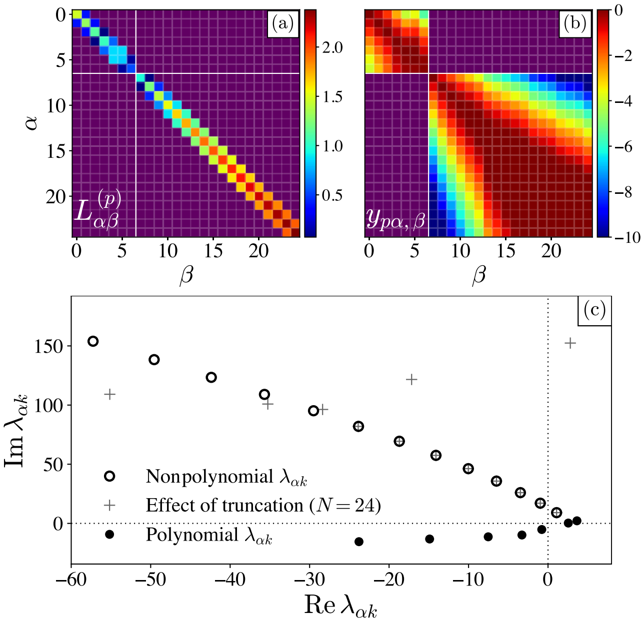

FIG. 4. Example of confluent Heun polynomial/nonpolynomial duality for polynomial order $p = 6$, and physical parameters $(s, \ell, m, n) = (-2, 2, 2, 6)$, $a/M = 0.7$, and $M\tilde{\omega}_{\ell mn} = 0.4239 - 1.0954i$. All color bars correspond to the $\log_{10}$ of the absolute values of quantities noted in annotation. Matrix elements of zero value are colored purple. Panel (a): matrix representation of the radial operator [Eq. (69)]. Panel (b): matrix representation of the radial operator's eigenvectors [Eq. (90)]. In panels (a) and (b), vertical and horizontal white lines delineate polynomial and nonpolynomial sectors. Panel (c): the radial operator's polynomial eigenvalues (filled circles) and the first 13 nonpolynomial eigenvalues (open circles).

monomials are the basis for power series expansions, but unlike the canonical confluent Heun polynomial, monomials are not an orthonormal basis, meaning that standard matrix interpretations do not apply for nonterminating series. Since the canonical confluent Heun polynomial are orthonormal, the polynomial and nonpolynomial sectors are clearly visible in Fig. 4(a).

At focus in Fig. 4(b) are the eigenvectors; rows labeled in α correspond to vectors $\vec{y}_{p\alpha}$. There, the polynomial solutions are shown as rows that have zero values after $\beta = 6$, as is equivalent to each confluent Heun polynomial only being comprised of canonical confluent Heun polynomials of order 6 and below. The nonpolynomial solutions are seen as the lower right-hand block, for which values are nonzero only for $\beta > 6$, i.e., the nonpolynomial solutions do not contain canonical confluent Heun polynomials with order $p \leq 6$.

Polynomial and nonpolynomial eigenvalues are shown in Fig. 4(c) as points in the complex plane. There, polynomial eigenvalues show a distinctly different distribution than their nonpolynomial counterparts. If a QNM is approximately polynomial as described in Sec. IV, then its eigenvalue distribution should be expected to also reflect polynomial/nonpolynomial duality.

D. QNM radial eigenvalue distributions

It was noted in Sec. IV that the $(\ell, m, n) = (2, 2, 6)$ QNM may be approximately polynomial for a BH spin of $a = 0.7$ (Table I). In particular, this QNM's upper pseudopolynomial order [Eq. (33)] is

$$p^{+}_{\star} = 6.2586 + 0.0743i. \tag{93}$$

Since the imaginary part of $p^{+}_{\star}$ is small, and the real part is close to 6 [cf. [Eq. (37)]], it is reasonable to expect rough agreement between that QNM's radial eigenvalues and the order-6 confluent Heun polynomial's polynomial *and* nonpolynomial eigenvalues (i.e., $p^{+}_{\star} \approx 6$).

In Fig. 5, the radial eigenvalue distributions for four select QNMs are shown. There, as n increases, so does the approximately polynomial sector of the eigenvalue distribution. The nearest confluent Heun polynomial eigenvalues have been added for comparison [see [Eq. (37)]]. For all cases, the qualitative features of the QNM eigenvalue distribution are captured by that of the confluent Heun polynomial eigenvalues. For example, the $n = 6$ QNM separation constant, A_{226}, is indeed well approximated by the dominant order-6 confluent Heun polynomial eigenvalue,

$$A_{226} \approx \mathrm{C}_0 + \mathrm{C}_1 + \lambda_{66}. \tag{94}$$

In Eq. (94), Eq. (31) has been restated in the current context, and the parameters, C_0 and C_1, have been computed with the relevant QNM frequency $\tilde{\omega}_{226}$. The fractional error between the left- and right-hand sides of Eq. (94) is 4.6%. A more thorough exploration of the QNM solution space is needed to determine whether the qualitative agreement in Fig. 5 is robust.

E. Validation of radial functions

When represented with canonical confluent Heun polynomials, the QNMs' radial problem may be written as

$$\mathcal{L}_{\xi}|f_n\rangle = A_n|f_n\rangle. \tag{95}$$

In Eq. (95), we have simply rewritten Eq. (13) with the overtone label, n, explicitly added. When represented with canonical confluent Heun polynomials, the radial functions, $f_n(\xi)$, are

$$|f_n\rangle = \sum_{k=0}^{\infty} |u_k\rangle\langle u_k|f_n\rangle. \tag{96}$$

In coordinate notation, this is simply

$$f_n(\xi) = \sum_{k=0}^{\infty} u_k(\xi)\langle u_k|f_n\rangle. \tag{97}$$

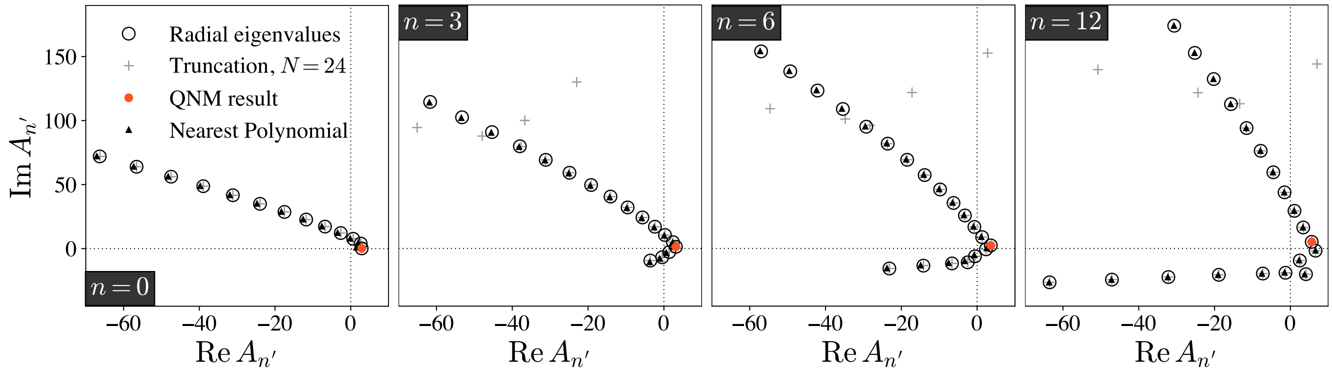

FIG. 5. Radial eigenvalue distributions for select quasinormal mode cases, all with BH dimensionless spin $a/M = 0.7$, and angular indices $(\ell, m) = (2, 2)$. In all panels, radial eigenvalues, $A_{n'}$, are noted with open circles, and the known QNM eigenvalue, $A_{\ell mn}$, is shown as a red filled circle (cf. Fig. 1). Left to right: radial eigenvalues for the respective $n \in \{0, 3, 6, 12\}$ QNM overtones. Respective absolute differences between known QNM eigenvalues (Refs. [125,126]) and those computed here (i.e., $|A_{\ell mn} - A_n|$) are $\{2.72 \times 10^{-9}, 4.72 \times 10^{-9}, 1.24 \times 10^{-9}, 6.28 \times 10^{-9}\}$. Eigenvalues for the confluent Heun polynomials with order $[\mathrm{Re}\, p_\star^+]$ [Eq. (37)] are shown by black triangles. Center right ($n = 6$): see panel (c) of Fig. 4 for comparison.

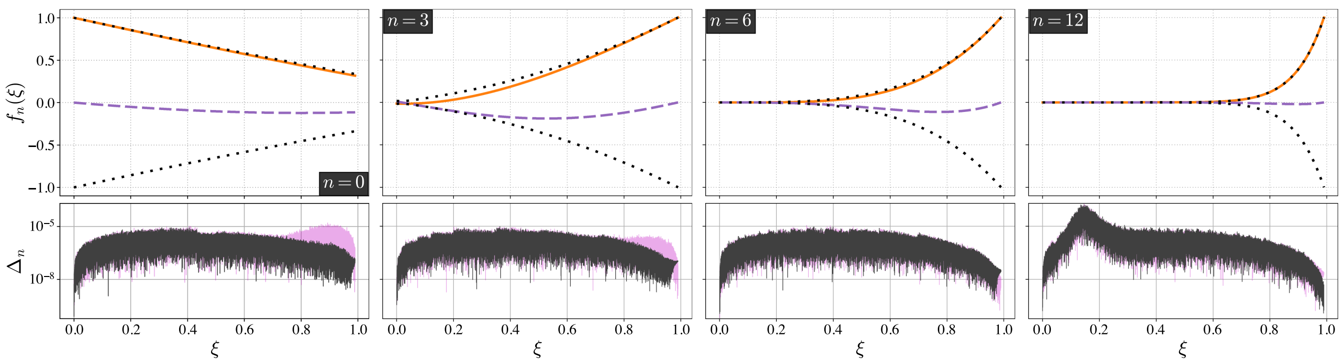

FIG. 6. Radial functions, $f_n(\xi)$, and related floating point error estimates, Δ_n, for the same cases shown in Fig. 5. Top row: the real part of each radial function, $\mathrm{Re} f_n(\xi)$, is denoted with a solid orange line. The imaginary part, $\mathrm{Im}\, f_n(\xi)$, is denoted with a dashed purple line, and the function's positive and negative magnitude, $\pm|f_n(\xi)|$ are denoted with dotted black lines. Bottom row: errors for each radial function, Δ_n [Eq. (98)]. In black are errors for $N = 24$, where all eigenvectors are consistent with the infinite dimensional problem. In magenta are errors for $N = 24$, where eigenvectors due to truncation are included. See Sec. VII for related discussion.

Upon solving the matrix eigenvalue problem [Eq. (59)], the accuracy of the each $f_n(\xi)$ may be quantified by

$$|(\mathcal{L}_\xi - A_n) f_n(\xi)| / |f_n(\xi)| = \Delta_n(\xi). \tag{98}$$

In Eqs. (98), (95) has been rearranged such that all quantities appear on the left-hand side. The absolute value has then been taken to yield a single real-valued error measure. If $f_n(\xi)$ are eigenfunctions, and the derivatives within $\mathcal{L}_\xi$ can be evaluated with infinite precision, then $\Delta_n(\xi)$ would equal zero for all values of ξ. In practice, $\Delta_n(\xi)$ will be very small relative to one and dominated by numerical noise.

In Fig. 6, example radial functions are shown along with their errors for the same QNM cases discussed in Fig. 5. There, errors have been computed using floating-point precision and spline interpolation for the derivatives [121,125]. Despite the result being significantly larger than the calculation's original precision, all cases are observed to have dimensionless errors on the order of 10^{-7}. In the top row of panels, radial functions have been scaled such that their largest absolute value is 1. There, it may be observed that as the overtone number increases, the relative value of the radial function at the BH event horizon appears to decrease, possibly implying tension with the physical (asymptotic) boundary conditions, which require $f_n(\xi)$ to be nonzero when $\xi \in \{0, 1\}$.

F. Schwarzschild and Kerr

Together, the previous examples enable the following observations. When considered for a single frequency parameter, $\tilde{\omega}$, the radial functions typically have distinct eigenvalues (Fig. 5), and so are linearly independent [74]. Although the space of eigenfunctions is countably infinite, finite dimensional truncations of this space may be solved for using canonical confluent Heun polynomials.

In practice, the radial functions will be finitely many and linearly independent and will therefore constitute a basis.

Further, due to the self-adjoint nature of the radial operator, with respect to the scalar product [Eq. (13)], the space of radial functions is orthogonal [54,110,127]. Since the canonical confluent Heun polynomial are an orthonormal basis, scalar products between different radial functions, $|f_p\rangle$ and $|f_q\rangle$, are equivalent to the simple vector dot product between their vector representations,

$$\langle f_p|f_q\rangle = \sum_{jk}\langle f_p|u_j\rangle\langle u_j|u_k\rangle\langle u_k|f_q\rangle \tag{99a}$$

$$= \sum_{k}\langle f_p|u_k\rangle\langle u_k|f_q\rangle \tag{99b}$$

$$= \vec{f}_p \cdot \vec{f}_q. \tag{99c}$$

Note that, in Eq. (99), canonical confluent Heun polynomials constitute spin-dependent bases. Note also that the radial functions may be normalized in the standard way, $|f_p\rangle \leftarrow |f_p\rangle/\sqrt{\langle f_p|f_p\rangle}$. In other words, when computed for a single frequency parameter, the radial functions define an orthonormal basis.

An important question in single BH perturbation theory is whether QNMs for one physical case may be used to efficiently represent QNMs in another. For example, it is common to represent the Kerr QNMs' angular functions in the basis of those for Schwarzschild [12,41,54,56,93,94]. Here, we are concerned with whether the same is true for the QNMs' radial functions. For simplicity, we will consider different BH spins, a single QNM frequency for each, and related families of single-frequency solutions to the radial equation. In effect, we ask whether there exists a mixing matrix between sets of radial functions derived from different BH spins.[12]

To answer this question, it cannot be avoided that, even for a single QNM, different values of BH spin correspond to different QNM frequencies [15,32,94,128]. When combined with the fact that all forms of Teukolsky's radial equation [Eq. (10)] are frequency dependent, this means that the QNM radial functions for different BH spins are members of different scalar product spaces. While a complete treatment of the question may require the use of a frequency-independent weight function, we remain free to apply *any* scalar product to the problem. Any choice of scalar product will impact the symmetry properties of $\mathcal{L}_\xi$ and the orthogonality properties of the radial functions.

Let the pth radial function for a given BH spin, a, be denoted $\vec{f}_p^{(a)}$. As mentioned previously, if $\vec{f}_p^{(a)}$ are defined with QNM frequency $\tilde{\omega}_{\ell mn}$, then $\vec{f}_n^{(a)}$ is the QNM's radial function. Since each a-dependent canonical confluent Heun polynomial basis is orthonormal, Eq. (99) may be interpreted to mean that the scalar product for all $\vec{f}_p^{(a)}$ is given by the right-hand side of Eq. (99c). Since the right-hand side of Eq. (99c) has no weight function, we may superficially conclude that the standard vector dot product is a frequency-independent scalar product of potential use.

Let the scalar product between a Schwarzschild (i.e., $a=0$) and Kerr radial function be

$$\vec{f}_p^{(0)} \cdot \vec{f}_q^{(a)} = \sum_k \left\langle f_p^{(0)} \middle| u_k^{(0)} \right\rangle \left\langle u_k^{(a)} \middle| f_q^{(a)} \right\rangle. \tag{100}$$

In Eq. (100), $u_k^{(a)}$ are canonical confluent Heun polynomials derived from a BH spin of a, where (s,l,m,n) are implicitly fixed. Further, bra-ket operations use the weight defined by the labeled spin value (e.g., $\langle f_p^{(0)}|u_k^{(0)}\rangle$ uses Eq. (14) defined with $a=0$). Vectors $\vec{f}_p^{(0)}$ and $\vec{f}_q^{(a)}$ will be considered normalized, making, e.g., the set of all $\vec{f}_p^{(0)}$ orthonormal. Therefore, the truncated set of Schwarzschild radial functions may constitute an orthonormal basis with a well-defined projection operator. The application of this projection operator to $\vec{f}_q^{(a)}$ is equivalent to the decomposition of a Kerr radial function onto the basis of Schwarzschild radial functions. This is

$$\vec{f}_q^{(a)} = \sum_{p=0} \vec{f}_p^{(0)} \left(\vec{f}_p^{(0)} \cdot \vec{f}_q^{(a)}\right). \tag{101}$$

In Eq. (101), $\vec{f}_p^{(0)} \cdot \vec{f}_q^{(a)}$ are elements of the mixing matrix between the Schwarzschild and Kerr radial functions. In the case of $a=0$, Eq. (101) simply reduces to $\vec{f}_q^{(a)} = \sum_{q=0} \vec{f}_p^{(0)} \delta_{pq}$, signaling a diagonal mixing matrix.

In Fig. 7, the $(s,\ell,m,n) = (-2,2,2,0)$ QNM frequencies have been used to compute Schwarzschild-Kerr mixing matrices for four values of BH spin.[13] As seen from left to right in Fig. 7, as BH spin increases, so too does the magnitude of off-diagonal matrix elements. Nevertheless, the mixing matrix appears to be approximately diagonal throughout the range of spins shown.

This result implies that there exists a one-to-one relationship between Schwarzschild and Kerr radial functions across a wide range of BH spins.

[12]Note that the invertibility of such a matrix was found to be a prerequisite to the existence of the adjoint-spheroidal harmonics presented in Ref. [56].

[13]The successful reproduction of Fig. 7 requires that one keep in mind the overall sign ambiguity discussed in Sec. V: Given canonical polynomials, $u_p^{(a)}$ and $u_p^{(a')}$, one can avoid the presence of an incongruous minus sign by using, e.g., the scalar product space of $u_p^{(a)}$ to compute the matrix whose diagonal elements are $\langle u_p^{(a)}|u_p^{(a')}\rangle$. Diagonal elements with a negative real part signal that $u_p^{(a')}$ should be scaled by -1.

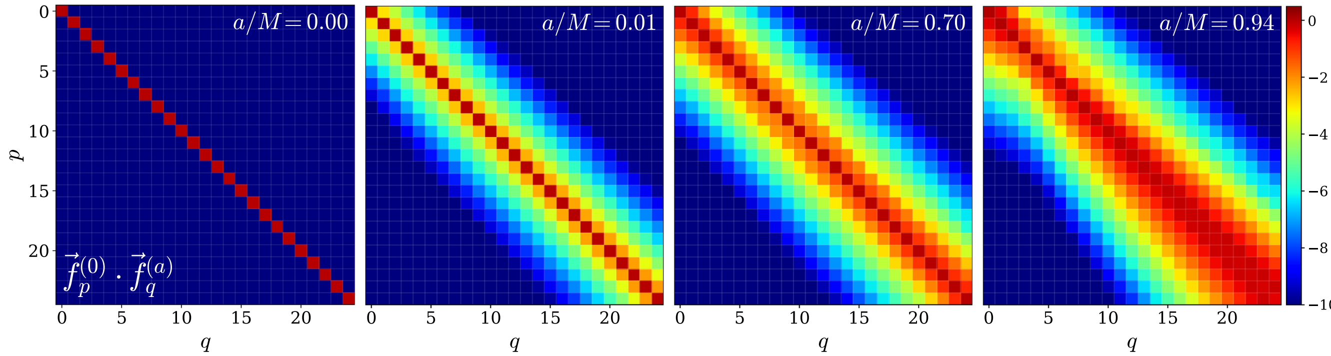

FIG. 7. Mixing matrices between Schwarzschild and Kerr radial functions for four values of BH spin: $a/M \in \{0, 0.01, 0.70, 0.94\}$. For each case, the first 24 radial functions have been computed using canonical confluent Heun polynomials derived from the $s = -2$, $(\ell, m, n) = (2, 2, 0)$ QNM frequencies; truncation effects have not been included. Different values of p and q correspond to different values of n' as discussed in Sec. III. Mixing matrices have been computed according to Eq. (100).

Such a one-to-one relationship is known to exist between the Schwarzschild and Kerr angular functions [56,94]. These functions are the spin weighted spherical and spheroidal harmonics, respectively [41,56,93,104,129]. It was found in Ref. [56] that the existence of a spherical-to-spheroidal mapping underpins the existence of another set of angular functions called adjoint-spheroidal harmonics, the significance of which may be understood thusly: Due to their different QNM frequencies, the QNMs' spheroidal harmonics are not orthogonal with each other; however, they are *bi*orthogonal with the adjoint-spheroidal harmonics. Therefore, the adjoint-spheroidal harmonics signal QNM orthogonality between modes of different ℓ. This perspective also defines the sense in which the QNMs are complete in ℓ [56].

In this context, Fig. 7 implies the potential biorthogonality and completeness of the QNMs' radial functions, i.e., the set of all QNM radial functions, where each radial function has frequency $\tilde{\omega}_{\ell mn}$, and where only n is allowed to vary. However, given the close relationship between the QNMs' radial functions and the confluent Heun polynomials, it is possible that the radial functions are not complete, but rather *overcomplete* (Sec. IV). Indeed, overcompleteness is perhaps most likely, given the known existence of QNM multiplets [41,130].

VIII. DISCUSSION AND CONCLUSIONS

The present work is based upon a simple premise: to solve Teukolsky's radial equation, rather than looking to special functions from other problems, we may need only look to the equation itself [54,108]. The result is a method for computing global solutions to the confluent Heun equation via a single expansion in polynomials that are natural to the problem. We have introduced such polynomials in Sec. V. In Sec. VI, we have shown that these polynomials enable the radial equation to be represented as a matrix that is both tridiagonal and symmetric. Lastly, in Sec. VII, we have demonstrated the use of these polynomials in various numerical examples, the last of which may be of particular relevance to the time-dependent perturbations of BHs [25–29]. We now briefly discuss connections and implications that have not been fully articulated thus far.

As noted previously, one of our goals has been to gain a deeper mathematical understanding of the QNM's radial problem. Consequently, our method for solving Teukolsky's radial equation is particular to the QNMs. If our method can be generalized to non-QNM boundary conditions, such as those of a point particle orbiting a BH, then new techniques of analysis and methods of evaluation may result. Concurrently, it may also be useful to reproduce our results for other formulations of BH perturbation theory and in more exotic spacetimes [40,131–133].

Of the techniques presented here, a number are open to refinement, further exploration, and connection with other recent results. For example, we have shown that, in some cases (particularly for large n), the QNM's separation constant is well approximated by the eigenvalue of a confluent Heun polynomial. We expect that more analytic understanding is tractable when either representing the problem in confluent Heun polynomials or their canonical counterparts. Further, there is good reason to think that more may be learned by a thorough comparison between our results and those known for Pollaczek-Jacobi polynomials [73,82,134,135]. There is also the possibility of combining the results presented here with recent iterative generalized spectral methods for computing QNM frequencies [75–79]. Regarding spectral pollution, it may also be possible to adapt techniques developed in quantum mechanics to mitigate the effect without incurring the added computational cost of increased basis size [97–100].

Lastly, one clear next step is to expand upon the results of Sec. VII to better understand whether the QNM's radial functions are complete. This would likely require a greater practical understanding of the complex-valued radial coordinate introduced in Paper I. Furthermore, this may require an analysis similar to that of Ref. [56] for the spheroidal harmonics. Intriguingly, if the QNM's radial functions are complete (in some practical way), then it would follow that any bounded spatial deviation from Kerr might be represented in terms of QNMs.

ACKNOWLEDGMENTS

The authors thank Katy Clough, Stephen Green, Scott Hughes, Laura Sberna, and Bernard Whiting for supportive discussions. L. L. was funded at King's College London by the Royal Society URF\R1\211451. M. F. was funded at King's College London by Royal Society enhancement Grant No. RF\ERE\210040 and by the King's College London department of physics.

[1] C. V. Vishveshwara, Phys. Rev. D **1**, 2870 (1970).
[2] B. P. Abbott *et al.* (LIGO Scientific Collaboration and Virgo Collaboration), Phys. Rev. Lett. **116**, 061102 (2016).
[3] B. P. Abbott *et al.* (Virgo Collaboration and LIGO Scientific Collaboration), Phys. Rev. Lett. **116**, 221101 (2016).
[4] R. Abbott *et al.* (LIGO Scientific Collaboration and Virgo Collaboration), Phys. Rev. X **11**, 021053 (2021).
[5] R. Abbott *et al.* (LIGO Scientific Collaboration, VIRGO Collaboration, and KAGRA Collaboration), Phys. Rev. X **13**, 041039 (2023).
[6] B. Abbott *et al.* (LIGO Scientific Collaboration and Virgo Collaboration), Phys. Rev. X **9**, 031040 (2019).
[7] S. A. Hughes, A. Apte, G. Khanna, and H. Lim, Phys. Rev. Lett. **123**, 161101 (2019).
[8] S. Khan, S. Husa, M. Hannam, F. Ohme, M. Pürrer, X. Jiménez Forteza, and A. Bohé, Phys. Rev. D **93**, 044007 (2016).
[9] S. Husa, S. Khan, M. Hannam, M. Pürrer, F. Ohme, X. Jiménez Forteza, and A. Bohé, Phys. Rev. D **93**, 044006 (2016).
[10] L. Pompili *et al.*, Phys. Rev. D **108**, 124035 (2023).
[11] W. H. Press, Astrophys. J. Lett. **170**, L105 (1971).
[12] W. H. Press and S. A. Teukolsky, Astrophys. J. **185**, 649 (1973).
[13] S. A. Teukolsky, Astrophys. J. **185**, 635 (1973).
[14] S. A. Teukolsky and W. H. Press, Astrophys. J. **193**, 443 (1974).
[15] E. Leaver, Proc. R. Soc. A **402**, 285 (1985).
[16] E. Berti, V. Cardoso, and C. M. Will, Phys. Rev. D **73**, 064030 (2006).
[17] L. London, D. Shoemaker, and J. Healy, Phys. Rev. D **90**, 124032 (2014).
[18] E. Hamilton, L. London, and M. Hannam, Phys. Rev. D **107**, 104035 (2023).
[19] G. Carullo *et al.*, Phys. Rev. D **98**, 104020 (2018).
[20] V. Baibhav, M. H.-Y. Cheung, E. Berti, V. Cardoso, G. Carullo, R. Cotesta, W. Del Pozzo, and F. Duque, Phys. Rev. D **108**, 104020 (2023).
[21] G. Carullo, W. Del Pozzo, and J. Veitch, Phys. Rev. D **99**, 123029 (2019); **100**, 089903(E) (2019).
[22] R. Cotesta, G. Carullo, E. Berti, and V. Cardoso, Phys. Rev. Lett. **129**, 111102 (2022).
[23] C. K. Mishra, K. G. Arun, B. R. Iyer, and B. S. Sathyaprakash, Phys. Rev. D **82**, 064010 (2010).
[24] S. Bhagwat, X. J. Forteza, P. Pani, and V. Ferrari, Phys. Rev. D **101**, 044033 (2020).
[25] M. Lagos and L. Hui, Phys. Rev. D **107**, 044040 (2023).
[26] S. R. Green, S. Hollands, L. Sberna, V. Toomani, and P. Zimmerman, Phys. Rev. D **107**, 064030 (2023).
[27] E. Cannizzaro, L. Sberna, S. R. Green, and S. Hollands, Phys. Rev. Lett. **132**, 051401 (2024).
[28] L. Sberna, P. Bosch, W. E. East, S. R. Green, and L. Lehner, Phys. Rev. D **105**, 064046 (2022).
[29] J. Redondo-Yuste, D. Pereñiguez, and V. Cardoso, Phys. Rev. D **109**, 044048 (2024).
[30] K. G. Arun *et al.* (LISA Collaboration), Living Rev. Relativity **25**, 4 (2022).
[31] A. Maselli, K. Kokkotas, and P. Laguna, Phys. Rev. D **95**, 104026 (2017).
[32] E. Berti, A. Sesana, E. Barausse, V. Cardoso, and K. Belczynski, Phys. Rev. Lett. **117**, 101102 (2016).
[33] E. Barausse, V. Cardoso, and P. Pani, J. Phys. Conf. Ser. **610**, 012044 (2015).
[34] A. Klein *et al.*, Phys. Rev. D **93**, 024003 (2016).
[35] M. Bailes *et al.*, Nat. Rev. Phys. **3**, 344 (2021).
[36] M. Vallisneri, J. Kanner, R. Williams, A. Weinstein, and B. Stephens, J. Phys. Conf. Ser. **610**, 012021 (2015).
[37] N. Karnesis *et al.*, Int. J. Mod. Phys. D **33**, 2450027 (2024).
[38] K. D. Kokkotas and B. G. Schmidt, Living Rev. Relativity **2**, 2 (1999).
[39] H.-P. Nollert, Classical Quantum Gravity **16**, R159 (1999).
[40] E. Berti, V. Cardoso, and A. O. Starinets, Classical Quantum Gravity **26**, 163001 (2009).
[41] G. B. Cook and M. Zalutskiy, Phys. Rev. D **90**, 124021 (2014).
[42] E. W. Leaver, J. Math. Phys. (N.Y.) **27**, 1238 (1986).
[43] E. W. Leaver, Phys. Rev. D **34**, 384 (1986).
[44] E. Berti, V. Cardoso, K. D. Kokkotas, and H. Onozawa, Phys. Rev. D **68**, 124018 (2003).
[45] E. Berti, V. Cardoso, and M. Casals, Phys. Rev. D **73**, 024013 (2006); **73**, 109902 (2006).
[46] E. Berti and V. Cardoso, Phys. Rev. D **74**, 104020 (2006).
[47] H. Yang, F. Zhang, A. Zimmerman, D. A. Nichols, E. Berti, and Y. Chen, Phys. Rev. D **87**, 041502 (2013).
[48] H. Yang, D. A. Nichols, F. Zhang, A. Zimmerman, Z. Zhang, and Y. Chen, Phys. Rev. D **86**, 104006 (2012).

[49] A. Zimmerman, H. Yang, F. Zhang, D. A. Nichols, E. Berti, and Y. Chen, arXiv:1510.08159.
[50] A. Zimmerman and Z. Mark, Phys. Rev. D **93**, 044033 (2016); **93**, 089905(E) (2016).
[51] M. Maggiore, Phys. Rev. Lett. **100**, 141301 (2008).
[52] N. Andersson, Phys. Rev. D **51**, 353 (1995).
[53] N. Andersson, Phys. Rev. D **55**, 468 (1997).
[54] L. T. London, preceding paper, Phys. Rev. D **113**, 044008 (2026).
[55] E. D. Fackerell and R. G. Crossman, J. Math. Phys. (N.Y.) **18**, 1849 (2008).
[56] L. T. London, Phys. Rev. D **107**, 044056 (2023).
[57] A. Ronveaux and F. Arscott, *Heun's Differential Equations*, Oxford Science Publications (Oxford University Press, New York, 1995).
[58] DLMF, *Solutions Analytic at Three Singularities: Heun Polynomials*, edited by F. W. J. Olver, A. B. Olde Daalhuis, D. W. Lozier, B. I. Schneider, R. F. Boisvert, C. W. Clark, B. R. Miller, B. V. Saunders, H. S. Cohl, and M. A. McClain, https://dlmf.nist.gov/, Release 1.1.10 of 2023-06-15.
[59] P. P. Fiziev, Phys. Rev. D **80**, 124001 (2009).
[60] S. Zarrinkamar and M. Hortaçsu, Adv. High Energy Phys. **2018**, 8621573 (2018).
[61] C. Dariescu, M.-A. Dariescu, and C. Stelea, Adv. High Energy Phys. **2021**, 5512735 (2021).
[62] A. P. Magnus, F. Ndayiragije, and A. Ronveaux, J. Approx. Theory **263**, 105522 (2021).
[63] O. Rosas-Ortiz and K. Zelaya, Ann. Phys. (N.Y.) **388**, 26 (2018).
[64] A. Mostafazadeh, J. Math. Phys. (N.Y.) **43**, 205 (2002).
[65] A. Andrianov, F. Cannata, and A. Sokolov, Nucl. Phys. B **773**, 107 (2007).
[66] E. Berti, V. Cardoso, and A. O. Starinets, Classical Quantum Gravity **26**, 163001 (2009).
[67] R. Zhang, H. Qin, and J. Xiao, J. Math. Phys. (N.Y.) **61**, 012101 (2020).
[68] D. C. Brody, J. Phys. A **47**, 035305 (2013).
[69] Y. Pinchover and J. Rubinstein, Equations in high dimensions, in *An Introduction to Partial Differential Equations* (Cambridge University Press, Cambridge, England, 2005), pp. 226–281.
[70] M. Abramowitz and I. A. Stegun, *Handbook of Mathematical Functions with Formulas, Graphs, and Mathematical Tables* (Dover, New York, 1964), 9th dover printing, 10th gpo printing ed.
[71] G. B. Arfken, H. J. Weber, and F. E. Harris, in *Mathematical Methods for Physicists (Seventh Edition)*, edited by G. B. Arfken, H. J. Weber, and F. E. Harris (Academic Press, Boston, 2013), 7th ed., pp. 401–445.
[72] R. Courant and D. Hilbert, *Methods of Mathematical Physics* (Wiley, New York, 1989).
[73] Y. Chen and D. Dai, J. Approx. Theory **162**, 2149 (2010).
[74] S. Axler, *Linear Algebra Done Right (eBook)* 3rd ed. (Springer, Cham, 2015).
[75] A. K.-W. Chung, P. Wagle, and N. Yunes, Phys. Rev. D **107**, 124032 (2023).
[76] J. L. Blázquez-Salcedo, F. S. Khoo, J. Kunz, and L. M. González-Romero, Phys. Rev. D **109**, 064028 (2024).
[77] A. K.-W. Chung, P. Wagle, and N. Yunes, Phys. Rev. D **109**, 044072 (2024).
[78] B. Ghojogh, F. Karray, and M. Crowley, arXiv:1903.11240.
[79] H. Zhu, J. L. Ripley, A. Cárdenas-Avendaño, and F. Pretorius, Phys. Rev. D **109**, 044010 (2024).
[80] G. Teschl, *Jacobi Operators and Completely Integrable Nonlinear Lattices*, Mathematical Surveys and Monographs (American Mathematical Society, Providence, 2000).
[81] A. B. J. Kuijlaars, A. Martinez-Finkelshtein, and R. Orive, Electron. Trans. Numer. Anal. **19**, 1 (2005); A. B. J. Kuijlaars, A. Martinez-Finkelshtein, and R. OrivearXiv:math/0301037
[82] Y. Chen, G. Filipuk, and L. Zhan, J. Math. Phys. (N.Y.) **60**, 113501 (2019).
[83] T. Chihara, *An Introduction to Orthogonal Polynomials*, Dover Books on Mathematics (Dover Publications, New York, 2011).
[84] L. Magaña Zertuche *et al.*, Phys. Rev. D **105**, 104015 (2022).
[85] J. L. Jaramillo, R. Panosso Macedo, and L. Al Sheikh, Phys. Rev. X **11**, 031003 (2021).
[86] V. Boyanov, V. Cardoso, K. Destounis, J. L. Jaramillo, and R. Panosso Macedo, Phys. Rev. D **109**, 064068 (2024).
[87] K. Destounis and F. Duque, *Black-Hole Spectroscopy: Quasinormal Modes, Ringdown Stability and the Pseudospectrum*, in: edited by E. Papantonopoulos and N. Mavromatos, Compact Objects in the Universe (Springer, Cham, 2024).
[88] A. Courty, K. Destounis, and P. Pani, Phys. Rev. D **108**, 104027 (2023).
[89] T. Torres, Phys. Rev. Lett. **131**, 111401 (2023).
[90] P. T. Leung, S. Y. Liu, and K. Young, Phys. Rev. A **49**, 3057 (1994).
[91] R. M. Wald, J. Math. Phys. (N.Y.) **20**, 1056 (2008).
[92] H. R. Beyer, J. Math. Phys. (N.Y.) **36**, 4815 (1995).
[93] S. O'Sullivan and S. A. Hughes, Phys. Rev. D **90**, 124039 (2014); **91**, 109901(E) (2015).
[94] E. Berti and A. Klein, Phys. Rev. D **90**, 064012 (2014).
[95] L. London and S. A. Hughes, arXiv:2206.15246.
[96] E. N. Petropoulou and L. Velázquez, J. Math. Anal. Appl. **420**, 852 (2014).
[97] L. Boulton, Applied Numerical Mathematics **99**, 1 (2016).
[98] M. Lewin and E. Séré, Proc. London Math. Soc. **100**, 864 (2010).
[99] E. B. Davies and M. Plum, arXiv:math/0302145.
[100] C. Martínez Adame, Math. Phys. Anal. Geom. **10**, 81 (2007).
[101] L. Blanchet, Living Rev. Relativity **17**, 2 (2014).
[102] R. H. Boyer and R. W. Lindquist, J. Math. Phys. (N.Y.) **8**, 265 (2004).
[103] E. Newman and R. Penrose, J. Math. Phys. (N.Y.) **3**, 566 (1962).
[104] E. T. Newman and R. Penrose, J. Math. Phys. (N.Y.) **7**, 863 (1966).
[105] M. Ruiz, R. Takahashi, M. Alcubierre, and D. Nunez, Gen. Relativ. Gravit. **40**, 2467 (2008).
[106] C. Merlin, A. Ori, L. Barack, A. Pound, and M. van de Meent, Phys. Rev. D **94**, 104066 (2016).

[107] B. F. Whiting, J. Math. Phys. (N.Y.) **30**, 1301 (1989).

[108] P. P. Fiziev, J. Phys. A **43**, 035203 (2009).

[109] E. Berti, J. Cardoso, V. Cardoso, and M. Cavaglia, Phys. Rev. D **76**, 104044 (2007).

[110] P. Lax, *Functional Analysis* (Wiley, New York, 2002).

[111] F. Finster and J. Smoller, Methods Appl. Anal. **23**, 35 (2016).

[112] C. García-Quirós, M. Colleoni, S. Husa, H. Estellés, G. Pratten, A. Ramos-Buades, M. Mateu-Lucena, and R. Jaume, Phys. Rev. D **102**, 064002 (2020).

[113] G. Kristensson, *Second Order Differential Equations—Special Functions and Their Classification* (Springer, Germany, 2010).

[114] H. T. Cho, A. S. Cornell, J. Doukas, and W. Naylor, Phys. Rev. D **80**, 064022 (2009).

[115] J. J. Sakurai, *Modern Quantum Mechanics (Revised Edition)* 1st ed. (Addison Wesley, Reading, MA, 1993).

[116] O. Christensen, *An Introduction to Frames and Riesz Bases* (Birkhäuser, Boston, 2003).

[117] R. Brito, V. Cardoso, and P. Pani, Lect. Notes Phys. **906**, 1 (2015).

[118] H. S. Vieira, V. B. Bezerra, and C. R. Muniz, Eur. Phys. J. C **82**, 932 (2022).

[119] M. Foucoin and L. London, Properties of natural polynomials for Kerr quasi-normal modes (to be published).

[120] W. Adkins and S. Weintraub, *Algebra: An Approach via Module Theory*, Graduate Texts in Mathematics (Springer, New York, 2012).

[121] C. R. Harris *et al.*, Nature (London) **585**, 357 (2020).

[122] T. mpmath development team, MPMATH: A Python library for arbitrary-precision floating-point arithmetic (version 1.3.0) (2023), http://mpmath.org/.

[123] P. Virtanen *et al.* (SciPy 1.0 Contributors), Nat. Methods **17**, 261 (2020).

[124] O. J. C. Dias and H. S. Reall, Classical Quantum Gravity **30**, 095003 (2013).

[125] L. London, E. Fauchon, and E. Hamilton, llondon6/positive: map, (2020).

[126] L. C. Stein, J. Open Source Softwaare **4**, 1683 (2019).

[127] R. Harvey, Math. Gaz. **39**, 719 (1955).

[128] L. London and E. Fauchon-Jones, Classical Quantum Gravity **36**, 235015 (2019).

[129] J. N. Goldberg, A. J. MacFarlane, E. T. Newman, F. Rohrlich, and E. C. G. Sudarshan, J. Math. Phys. (N.Y.) **8**, 2155 (1967).

[130] A. Maassen van den Brink, J. Math. Phys. (N.Y.) **45**, 327 (2004).

[131] Y. Mino, M. Sasaki, M. Shibata, H. Tagoshi, and T. Tanaka, Prog. Theor. Phys. Suppl. **128**, 1 (1997).

[132] S. A. Hughes, Phys. Rev. D **62**, 044029 (2000); **67**, 089902 (2003).

[133] J. L. Ripley, Classical Quantum Gravity **39**, 145009 (2022).

[134] C. Min and Y. Chen, Math. Models Methods Appl. Sci. **46**, 15270 (2023).

[135] J. Yu, C. Li, M. Zhu, and Y. Chen, J. Math. Phys. (N.Y.) **63**, 063504 (2022).